Scribble Subcellular Localization Modulates Recruitment of Distinct YES1 Conformations to Regulate YAP Phosphorylation

by

Dongyu Zhao

A dissertation submitted in partial fulfillment
of the requirements for the degree of
Doctor of Philosophy
(Chemical Biology)
in the University of Michigan
2020

Doctoral Committee:

Assistant Professor Brent R. Martin, Co-Chair
Associate Professor Bruce Palfey, Co-Chair
Associate Professor Jayakrishnan Nandakumar
Associate Professor Zaneta Nikolovska-Coleska
Professor Nils G. Walter

Dongyu Zhao

donyu@umich.edu

ORCID iD: 0000-0003-3619-8197

Dedication

I dedicate this dissertation to all my friends, mentors and families.

Acknowledgements

First, I would like to thank my mentor Dr. Brent Martin for his patient guidance and continuous support for my PhD studies and future careers, I will be forever grateful. Brent is a brilliant scientist with integrity and passion. He has impressed me with his knowledge and critical thinking in science. He put his trust in me since the very first day I joined his outstanding group. His hands-off approach was instrumental in allowing me to become an independent researcher. Whenever I meet with difficulties, he is always willing to lend me a hand. I feel so fortunate to have Brent as my mentor during my graduate life.

I would like to acknowledge my committee members, Dr. Bruce Palfey, Dr. Jayakrishnan Nandakumar, Dr. Nils G. Walter and Dr. Zaneta Nikolovska-Coleska, for critical feedback and providing valuable guidance and constructive suggestions over the past three years. I also want to thank Dr. Stephen Weiss for his valued guidance during my rotation and for generous help during my PhD studies.

I also want to thank all current members and alumni in Martin lab, who created a wonderful environment in which to do research. To mention a few, I would like to thank Dr. Bo Peng for providing invaluable guidance in the synthesis. Dr. Sarah Haynes for mass spectrometry support. Dr. Yu Hsuan Kuo and John Crellin for their support and bringing fun to my journey to PhD.

I want to thank Zhangyuan Yin, I am grateful that he never got too mad at me for requesting dozens of Western blots. The conversations with him helped me a lot in my research and brought me a lot of joy and happiness.

Additionally, I would like to thank the Rackham Graduate school for providing me with the predoctoral research grant for my thesis. I would like to thank the Chemical Biology Program for the support throughout the years. Laura and Traci, thank you for providing assistance in the past five years.

Last, but most importantly, I want to thank the love and support from my family, my parents, my sister, my wife, who are my motivation.

Table of Contents

List of Tables

List of Figures

List of Appendices

.

Abstract

The multi-domain scaffolding protein Scribble regulates cell polarity and growth signaling at cell-cell junctions. In epithelial cancers, its mislocalization and overexpression paradoxically transforms Scribble from a tumor suppressor to a driver of tumorigenesis. Here we profiled Scribble protein-protein interactions to identify regulators of mislocalized Scribble-driven tumorigenesis. Scribble-HaloTag fusion cells were generated by CRISPR-Cas9 genome editing. Expression of the epithelial-to-mesenchymal transcription factor (EMT-TF) Snail displaced Scribble-HaloTag from the plasma membrane, mirroring the mislocalization observed in cancers. Halo-ligand affinity purification coupled with mass spectrometry analysis identified the Src-family kinase YES1 as a mislocalized Scribble interaction partner, preferentially recruiting the active, αC-helix-in (or open) conformation. Furthermore, Snail expression promotes Yes-associated kinase-1 (YAP) nuclear localization independent of the hippo pathway, while Scribble HaloPROTAC degradation and siRNA knockdown each attenuate YAP-Y357 phosphorylation. Altogether, mislocalized Scribble recruits conformationally open YES1 to promote YAP phosphorylation, linking Scribble mislocalization to amplified growth signaling. This study reveals a novel role of Scribble in the regulation of YES1-YAP oncogenic signaling pathway, identifies one of the mechanisms underlying dysregulated Hippo signaling components contribute to the tumorigenesis, and underpins the importance of proper cellular subcellular localization to a tumor suppressor protein.

Chapter 1 Introduction

Introduction

In epithelial cells, maintenance of apical-basolateral polarity gradients by distinct molecular complexes ensures appropriate contact inhibition and spatially defined proliferation. The conserved polarity protein Scribble was first identified in Drosophila as a multi-functional tumor suppressor regulating epithelial apical-basolateral polarity, junctional integrity, proliferation, and metastasis. In normal polarized epithelial cells, Scribble localizes to cell-cell junctions to maintain epithelial integrity, suppress cell overgrowth, and prevent tumorigenesis (Humbert et al., 2008). In human cancers, Scribble is mislocalized largely to the cytosol and overexpressed, (Feigin et al., 2014; Liu et al., 2017; Vaira et al., 2011; Zhan et al., 2008) where it synergizes with oncogenic signals to enhance tumorigenesis (Cordenonsi et al., 2011; Feigin et al., 2014; Liu et al., 2017; Wan et al., 2018; Zhan et al., 2008). This redistribution is in-part orchestrated by suppression of protein acyl transferases and elevated depalmitoylase activity that together reduce Scribble S-palmitoylation. In mouse models, Scribble deletion is lethal, yet heterozygous mice exhibit defective epithelial cell polarity, widespread hyperplasia, and enhanced tumorigenesis (Pearson et al., 2011; Zhan et al., 2008; Zhou et al., 2016). When mutated to restrict localization to the cytosol, MMTV-driven Scribble over-expression sequesters PTEN in the cytoplasm, leaving membrane-localized AKT signaling unchecked. Accordingly, Scribble has distinct functions and potentially unique protein-protein interactions in different cellular compartments, acting to suppress growth signals at the basolateral membrane, while

exacerbating growth signals in the cytosol. Since Scribble also suppresses MAPK, YAP/TAZ, and other prominent oncogenic pathways, a more detailed map of context-dependent interactions could provide new insights.

YES1 is a non-receptor tyrosine kinase belongs to the Src family kinase (SFK) (Sen and Johnson, 2011). Like other SFK members, YES1 undergoes large conformation rearrangement to switch from 'closed' inactive state to 'open' active states upon activation by cellular signals (Boggon and Eck, 2004). As a proto-oncogene, both YES1 expression and kinase activity are precisely controlled in normal cells. Deregulation of YES1 is related to enhanced cell proliferation (Garmendia et al., 2019; Hamamura et al., 2011; Sato et al., 2012; Tan et al., 2015; Yeung et al., 2013), cell migration and invasion (Barraclough et al., 2007; Hamamura et al., 2011; Jin et al., 2016; Kleber et al., 2008; Tauzin et al., 2011), metastasis (Chatterji et al., 2015) and chemotherapy resistance (Chen et al., 2018; Fan et al., 2018; Takeda et al., 2017; Touil et al., 2014; Wan et al., 2015) in a variety of cancers. Although gene amplification and elevated transcription partially explain how YES1 is overexpressed in cancer cells (Fan et al., 2018; Singh et al., 2019), the knowledge of how its kinase activity is upregulated remains incomplete and unclear. Recent studies show that heat stress and cytokines can elicit YES1 activation (Fan et al., 2019; Liang et al., 2013). However, whether such effects also exist in cancer is unknown.

The Domain Structure of Scribble

Although originally identified in *Drosophila*, the structure of Scribble is conserved among different species. It is a member of the LAP (leucine rich repeats and PDZ domain) protein family. The human Scribble protein consists of 1630 amino acids and contains three major function domains: N-terminal region composed of sixteen leucine rich repeats (LRRs) and

four PDZ (PSD-95/Disc large/Zonula occludens-1) domains; C-terminal region with no identified protein domain (**Figure 1.1**).

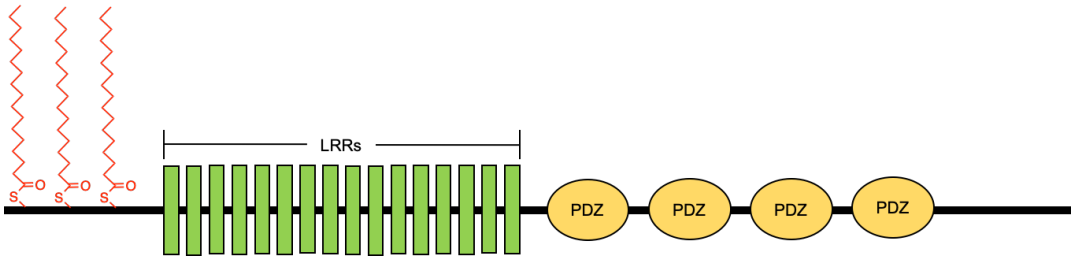

Figure 1.1 The functional domains of Scribble.

Leucine rich repeat (LRR) is a protein recognition motif consisting of 20 to 30 amino acids stretch rich in leucine. LRRs fold into an alpha-beta horseshoe shape and mediate protein-protein interactions (PPIs) in numerous proteins (Enkhbayar et al., 2004). However, there is few known Scribble interactors that associate through LRRs. Instead, LRRs are required for the membrane targeting of Scribble, which is essential for Scribble function (Albertson et al., 2004; Navarro et al., 2005). Mutating a conserved proline to leucine (P305L) within the LRR region totally abolishes Scribble membrane localization (Audebert et al., 2004). Apart from the LRR domains, Scribble membrane localization is also regulated by S-palmitoylation at evolutionarily conserved N-terminal cysteine residues (Chen et al., 2016).

The PDZ domain is also a common protein-protein interaction module that plays a central role in orchestrating multiple intracellular signaling pathways. The mode of how a PDZ domain recognizes its target protein has been well characterized, generally involving PDZ binding to the very last four amino acids at the C-terminus of the target protein (Lee and Zheng, 2010). Based on the sequence, PDZ binding motifs can be grouped into three major classes: X-S/T-X-hydrophobic-COOH for Class I; X-hydrophobic-X-hydrophobic-COOH for Class II and X-D/E-

X-hydrophobic for Class III (von Nandelstadh et al., 2009). Moreover, the PDZ binding motif phosphorylation has also been reported to affect PDZ binding (Sundell et al., 2018). Large-scale interaction profiling of PDZ domains using peptides identified that the Scribble PDZ binding motif belongs to Class I (Ivarsson et al., 2014). To date, most of the identified interactors associate with Scribble via their PDZ binding motifs (Bonello and Peifer, 2019), suggesting PDZ domains are crucial for the adaptor function of Scribble.

Although no C-terminal protein domain has been identified, Scribble's C-terminal region still mediates a few interactions such as with β2-spectrin (Boeda and Etienne-Manneville, 2015), ERK (Nagasaka et al., 2010b), PP1γ (Nagasaka et al., 2013) and Sema4A (Sun et al., 2017).

The Function of Scribble in Normal Cells

As a multi-domain scaffolding protein, the function of Scribble in a specific biological context is determined by the subcellular localization and the assembly of multiprotein complexes. In normal cells, Scribble is involved in the regulation of diverse cellular processes including maintenance of apical-basolateral cell polarity (Bilder and Perrimon, 2000), neural development and function (Moreau et al., 2010; Sun et al., 2009; Sun and Bamji, 2011), asymmetric cell division (Albertson and Doe, 2003; Mohr et al., 2018; Pham et al., 2015), cell proliferation (Halder and Johnson, 2011; Nagasaka et al., 2010a; Young et al., 2013) and migration (Dow et al., 2007; Michaelis et al., 2013; Osmani et al., 2006; Sun et al., 2017).

Scribble was first identified in *Drosophila* regulating epithelial apical-basolateral polarity and junctional integrity (Bilder and Perrimon, 2000). To maintain apical-basolateral polarity, Scribble localizes at the cell-cell junctions such as adhere junctions and tight junctions, establishing Scribble/Dlg/Lgl polarity module that mutually antagonizes the basolateral diffusion of apical determinants such as Crumbs, aPKC, and Par proteins (Grifoni et al., 2007; Grzeschik

et al., 2010). In epithelial cells, the maintenance of apical-basolateral polarity gradients by distinct protein complexes ensures appropriate contact inhibition and spatially defined proliferation. Loss of Scribble or its junctional localization leads to the disruption of apical-basolateral polarity.

A synapse, also called neuronal junction, is a unique subcellular organelle in the nervous system. A neuron uses synapses to transmit signals to another neuronal cell or to a target effector cell, thus synapses are regarded as specialized cell-cell junctions in the nervous system. Scribble localization at the synapse has also been reported (Moreau et al., 2010; Sun et al., 2009). At the synapse, Scribble/ β-catenin/cadherin complex recruits β-PIX, a Rac/Cdc42 guanine nucleotide exchange factor (GEF), to stimulate local actin polymerization and recruit synaptic vesicles (Sun and Bamji, 2011). Loss of Scribble affects synaptic maturation and pruning, resulting in changed learning and memory abilities and impaired social behavior (Moreau et al., 2010).

Scribble also plays an important role in asymmetric cell division, a process in which a progenitor cell divides asymmetrically to generate two daughter cells with different cellular fates (Mohr et al., 2018; Pham et al., 2015). To accomplish this progress, the progenitor cell must be apical-basolateral polarized, orient and align the spindle with the axis of polarity, and distribute the cell fate determinants asymmetrically along with the spindle (Knoblich, 2010). Mutation or deletion of Scribble impairs this process, leading to the altered cell fates (Albertson and Doe, 2003; Mohr et al., 2018; Pham et al., 2015). The exact mechanism by which Scribble regulates asymmetric cell division remains unclear.

Tumor suppressor proteins are proteins that regulate cell division and replication. As a tumor suppressor, Scribble directly regulate signaling pathways that control cell proliferation. For instance, Scribble suppresses ERK signaling through a direct interaction with ERK that

restricts ERK on the membrane, resulting in reduced ERK phosphorylation and nuclear translocation (Nagasaka et al., 2010a). Moreover, Scribble can inhibit ERK signaling activation by recruiting PP1α away from Shoc2 to decrease Raf activation (Young et al., 2013). On the other hand, loss of Scribble also cooperates with oncogenic Ras to promote ERK signaling and enhance tumorigenicity (Dow et al., 2008; Wu et al., 2010). Without its plasma membrane localization, Scribble-mediated tumor suppression of Ras/MAPK-driven cell growth are lost. Besides ERK signaling, Scribble also participates in the Hippo signaling pathway, a highly conserved pathway that governs organ size through the regulation of cell proliferation and apoptosis (Halder and Johnson, 2011). One crucial event mediated by the Hippo signaling pathway is the phosphorylation and inhibition of transcription co-activators YAP and TAZ. At the molecular level, Scribble bridges YAP/TAZ between LATS and MST to promote YAP/TAZ phosphorylation, leading to YAP/TAZ cytoplasmic accumulation and degradation (Cordenonsi et al., 2011; Xu et al., 2018). Loss of Scribble leads to increased YAP/TAZ nuclear localization and transcriptional activity.

Scribble also exerts pro-migration function in diverse cell types including astrocytes (Osmani et al., 2006), MCF-10A epithelial cells (Dow et al., 2007), dendritic cells (Sun et al., 2017) and endothelial cells (Michaelis et al., 2013). The regulatory role of Scribble played in the Rho GTPase activity underlies the mechanism of Scribble mediated cell migration.

Dysregulation of Scribble in Cancer

Cells generally grow to a dense monolayer and stop growing, a phenomenon mediated by a process termed ‘contact inhibition’, but is biochemically defined by the recruitment of growth suppressors to cell-cell junctions. In polarized cells, Scribble localizes to the basolateral membrane (Dow et al., 2003). In contrast, Scribble is mislocalized to the cytoplasm in most

epithelial cancers (Feigin et al., 2014). While Scribble is not widely mutated in cancers, its mislocalization and amplification are clinically correlated with high-grade cervical carcinomas (Nakagawa and Huibregtse, 2000; Nakagawa et al., 2004), as well as malignant colon (Gardiol et al., 2006), prostate (Pearson et al., 2011), breast (Zhan et al., 2008), and other epithelial cancers (Vaira et al., 2011). Overall, Scribble mislocalization away from cell-cell junctions is highly correlated with poor survival in human cancers. Several classes of viruses employ mechanisms to bypass Scribble repression. The papilloma viral protein E6 binds Scribble directly, targeting it for ubiquitination and degradation (Nakagawa and Huibregtse, 2000). Similarly, the retroviral protein Tax and the avian influenza virus protein NS1 each re-localize Scribble to the cytosol (Arpin-Andre and Mesnard, 2007; Liu et al., 2010). In addition, Scribble $^{+/-}$ heterozygous male mice develop widespread epithelial hyperplasia (Pearson et al., 2011), and MMTV-driven conditional knockout of Scribble in female mice induces breast hyperplasia and widespread tumor formation (Feigin et al., 2014).

The Domain Structure and Regulation of YES1 Kinase

YES1 is a member of the Src family of protein tyrosine kinases (SFKs), a family of kinases that play key roles in regulating cell morphology, motility, proliferation, and survival. In humans, SFK family has 11 members and including Blk, Brk, Fgr, Frk, Fyn, Hck, Lck, Lyn, Src, Srm, and Yes1, among which YES1 is expressed in all cell types (Thomas and Brugge, 1997). All the members are structurally related and share a conserved domain structure. In this thesis, I will only address the structure and function of YES1.

From its N-terminus to its C-terminus, YES1 consists of an N-terminal myristoyl group attached to an SH4 domain, a YES1 unique domain, an SH3 domain, an SH2 domain, a protein–tyrosine kinase domain, and a C-terminal regulatory segment (**Figure 1.2**). YES1 also contains a

cysteine residue downstream of the myristylated glycine that gets palmitoylated (Sandilands et al., 2007; Schindler et al., 1999).

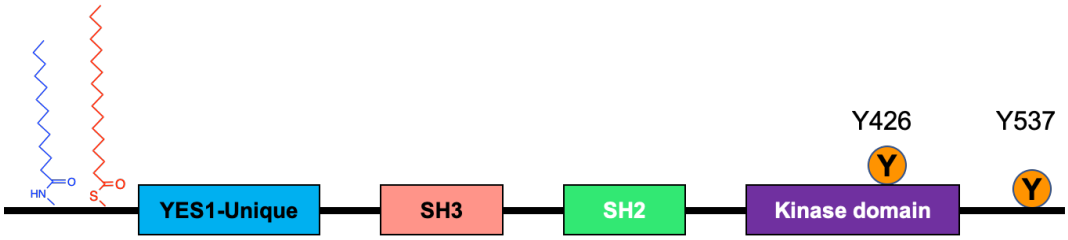

Figure 1.2 The functional domains of YES1 kinase.

Myristylation and palmitoylation in SH4 domain facilitate the attachment of YES1 to the membranes. SH3 and SH2 domains are involved in the substrate recognition in which SH3 domain recognizes proline-rich sequences bearing 'PXXP' motif and SH2 domain recognizes phosphor-tyrosine. Moreover, the intramolecular interactions between SH3 and SH2 domains restrict the activity of YES1 (Brown and Cooper, 1996). YES1 kinase domain shares the characteristic bilobed protein kinase architecture (Schindler et al., 1999; Williams et al., 1997; Xu et al., 1997). Residues 277–347 make up the small amino-terminal lobe of YES1 kinase and residues 351–530 make up the large carboxyl-terminal lobe. The smaller lobe consists primarily of antiparallel β-sheet structure and is mainly involved in ATP binding. The larger lobe consists primarily of α-helix and is responsible for binding the substrate. The catalytic site of YES1 is located at the cleft between the two lobes. The cleft forms an activation loop that contains Tyrosine Y426 which is the positive regulatory site responsible for maximizing kinase activity (Brown and Cooper, 1996). The movements of the two lobes with respect to one another can open or close the cleft. The kinase domain adopts open form to allow access of ATP to the catalytic site and release of ADP, while adopts closed form to bring catalytic residues close to

the catalytic site. The short C-terminal tail of YES1 contains an autoinhibitory phosphorylation site (Tyr 537), which plays an important role in the regulation of YES1 kinase activity.

Like other Src family kinase members, YES1 is in a dynamic equilibrium between inactive and active forms (Tatosyan and Mizenina, 2000). Active YES1 adopts open configuration in which Tyr 537 is dephosphorylated while Tyr 426 is autophosphorylated (**Figure 1.3B**). In contrast, inactive YES1 adopts a closed and compact configuration. The C-terminal phosphorylated Tyr 537 interacts with SH2 domain, which blocks the access of external ligands, results in a closed and compact configuration. Several kinases and phosphatases are involved in the regulation of Tyr 537 phosphorylation. In the closed configuration, the activation loop fills the catalytic cleft and masks Tyr 426 residue, preventing Tyr 426 autophosphorylation and subsequent activation (**Figure 1.3A**).

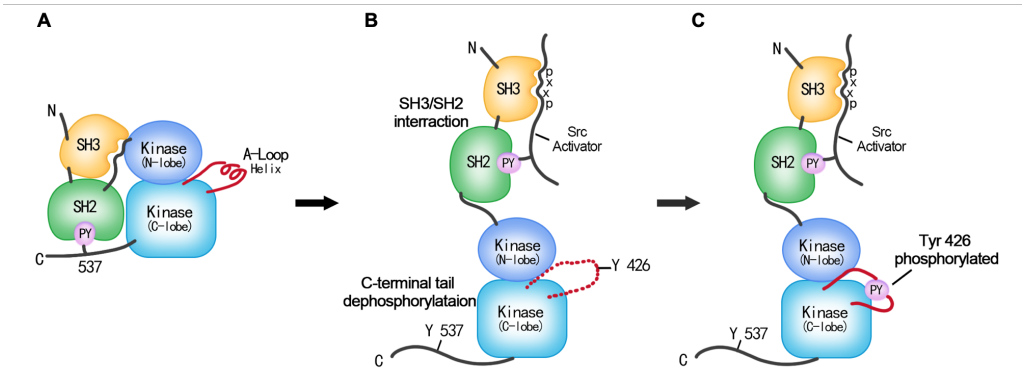

Figure 1.3 The domain structure of YES1 kinase.

(A) The restrained conformation of YES1 is stabilized by intramolecular interactions among the kinase domain, the SH2/SH3 domains, and the phosphorylated C-terminal tail. (B) Displacement of SH2 and/or SH3 domains induces YES1 to adopt open configuration. (C) Phosphorylation of Tyr-426 initiates a conformational reorganization of the whole activation loop, resulting a fully active tyrosine kinase.

Involvement of YES1 in Cancer

There are tremendous studies demonstrating that YES1 kinase activity or protein levels are elevated in many cancers, including non-small cell lung cancer (NSCLC) (Garmendia et al., 2019), basal-like breast cancer (Bilal et al., 2010), rhabdomyosarcoma (Yeung et al., 2013), colon carcinoma (Sancier et al., 2011), brain-metastatic melanomas (Marchetti et al., 1998) and malignant mesothelioma (Sato et al., 2012) et al. YES1 actions in cancer cells are pleiotropic including effects on cell proliferation (Garmendia et al., 2019; Hamamura et al., 2011; Sato et al., 2012; Tan et al., 2015; Yeung et al., 2013), migration and invasion (Barraclough et al., 2007; Hamamura et al., 2011; Jin et al., 2016; Kleber et al., 2008; Tauzin et al., 2011), metastasis (Chatterji et al., 2015) and chemotherapy resistance (Chen et al., 2018; Fan et al., 2018; Takeda et al., 2017; Touil et al., 2014; Wan et al., 2015).

YES1 plays an important role in cancer cell proliferation. Downregulation of YES1was found to inhibit cell proliferation in several cancer cells (Bilal et al., 2010; Fang et al., 2017; Shen et al., 2019; Tan et al., 2015). Recent studies have demonstrated that one of mechanisms that underlie YES1-promoted cancer cell proliferation is through the YES1-induced phosphorylation of YAP at Tyr 357, which fosters YAP nuclear localization and the formation of YAP-TBX5-beta-catenin complex to promote cell survival and proliferation (Rosenbluh et al., 2012).

One of the key processes in metastasis is the increased cell migration in cancer cells (Friedl and Wolf, 2003). YES1 can promote this process by mediating PI3K/AKT signaling pathway in ovarian cancer cells (Jin et al., 2016). The exact mechanisms underlying the YES1-promoted cancer cell migration and metastasis are still obscure.

At present, chemotherapy is still the standard of care to treat many cancers. However, cancer cells have evolved a variety of mechanisms to evade the effects of chemotherapeutic agents, such as inactivation of drugs (Michael and Doherty, 2005), multi-drug resistance (MDR) (Zahreddine and Borden, 2013), inhibition of cell apoptosis (Mohammad et al., 2015), changes to the drug metabolism (Zaal and Berkers, 2018), enhanced the DNA repair and gene amplification (Rocha et al., 2018), and epigenetic altering (Zeller and Brown, 2010). Recent studies have demonstrated that *YES1* amplification is a mechanism by which cancer cells use to counteract the effects of inhibitors targeting EGFR (Fan et al., 2018) and HER2 (Takeda et al., 2017).

In this thesis, we hypothesize that mislocalization of Scribble results in aberrant, disease-contributing interactions. In the following chapters, we use multiple chemical biology approaches to address this question. We develop a genetically induced epithelial cancer model in which Scribble is mislocalized. Using this engineered cancerous cell line, we reveal a novel role of Scribble in the regulation of YAP-Y357 phosphorylation through interaction with YES1 kinase. Furthermore, we discover that membrane associated Scribble are preferentially interact with inactive YES1, while cytosolic Scribble can only interact with active YES1. This work is important for the field of cancer biology as it identifies a dysregulated crosstalk between tumor suppressor genes and oncogenes.

Chapter 2 Profiling Scribble Downstream Regulators in Engineered Cancer Model

Abstract

The multi-domain scaffolding protein Scribble regulates cell polarity and growth signaling at cell-cell junctions. Dysregulation of Scribble is commonly observed in many epithelial cancers. This dysregulation paradoxically transforms Scribble from a tumor suppressor to a driver of tumorigenicity. To profile the downstream regulators of the cell polarity regulator Scribble, we use multiple chemical biology approaches including CRISPR-Cas9 mediated genome editing, PROTAC degradation, TMT quantitative proteomics, protein engineering, small molecule inhibitors plus biochemical and cellular assays to address fundamental questions in cell biology. Through our efforts, we discovered a novel Scribble interaction partner linking Scribble localization to YAP activation.

Introduction

Originally identified in Drosophila, the cell polarity tumor suppressor Scribble has emerged as a central regulator of cell growth, invasion, and malignancy (Bilder and Perrimon, 2000; Dow et al., 2003; Feigin et al., 2014). In normal polarized epithelial cells, Scribble is mainly localized at cell-cell junctions such as adhere junctions and tight junctions, forming Scribble/Dlg/Lgl polarity module to control tumorigenesis (Humbert et al., 2008). Although anchored on the plasma membrane via palmitoylation (Chen et al., 2016; Hernandez et al., 2017), Scribble membrane localization is not static. Previous work has shown that Scribble translocates between basal and lateral membrane during differentiation, implying that its function

on the membrane is tightly regulated under temporal and spatial dimensions (Hartleben et al., 2012). Loss of Scribble results in epithelial mesenchymal transition (EMT) (Lamouille et al., 2014), a process by which epithelial cells lose their cell polarity and cell-cell junction, leads to tumor initiation and progression (Pearson et al., 2011; Zhan et al., 2008; Zhou et al., 2016). However, in many malignant epithelial cancers, Scribble is overexpressed and accumulated in the cytoplasm (Feigin et al., 2014; Liu et al., 2017; Vaira et al., 2011; Zhan et al., 2008). Many studies have demonstrated that cytoplasmic localization of Scribble promotes tumorigenesis (Cordenonsi et al., 2011; Feigin et al., 2014; Liu et al., 2017; Wan et al., 2018; Zhan et al., 2008). Interestingly, although loss of cell-cell junction and polarity is commonly observed in malignant tumors of epithelial origin (Coradini et al., 2011), a significant portion of Scribble is still associated with cell membrane in these cancer cells. Thus, one neglected, seemingly redundant but fundamental question needs to be answered: as cell-cell junction is disrupted and proteins diffuse freely on the membrane in malignant cancer cells (Su et al., 2012), does the remaining membrane associated Scribble can still function as a tumor suppressor?

In this study, we implement a genetically induced epithelial cancer model strategy to profile Scribble downstream regulators by combining chemical biology approaches including CRISPR-Cas9 mediated genome editing, HaloPROTAC degradation, TMT quantitative proteomics, plus biochemical and cellular assays, for the first time we discovered that Scribble interacts with YES1 in a subcellular localization dependent way. Using configuration specific Src kinase inhibitors, we further identified that YES1 adopts different configurations to interact with membrane associated, but tight junction excluded Scribble and its cytosolic counterpart. These findings demonstrate that mislocalized Scribble plays a dual role in the regulation of YES1 kinase oncogenic pathway.

Results

The MDCK cell line is widely used as a model in the field of epithelial research as they demonstrate clear apical-basolateral cell polarity and form well defined tight junctions (Dukes et al., 2011). We and many others previously reported that Scribble is localized at tight junctions and functions as a tumor suppressor in MDCK cells (Chen et al., 2016; Dow et al., 2003; Golebiewski et al., 2011; Hernandez et al., 2017; Ivanov et al., 2010; Nagasaka et al., 2006; Navarro et al., 2005; Qin et al., 2005). Therefore, we choose MDCK as our parental cell line to create the epithelial cancer model. Since MDCK is a hard-to-transfect cell line (Schuck et al., 2004), to overcome the low efficiency of homology directed recombination (HDR), we took the advantage of two-step CRISPR-Cas9 genome editing strategy (**Figure 2.1**) to knock in HaloTag on the C-terminus of Scribble (Xi et al., 2015). The workflow to generate this cell line is described in detail in **Methods**.

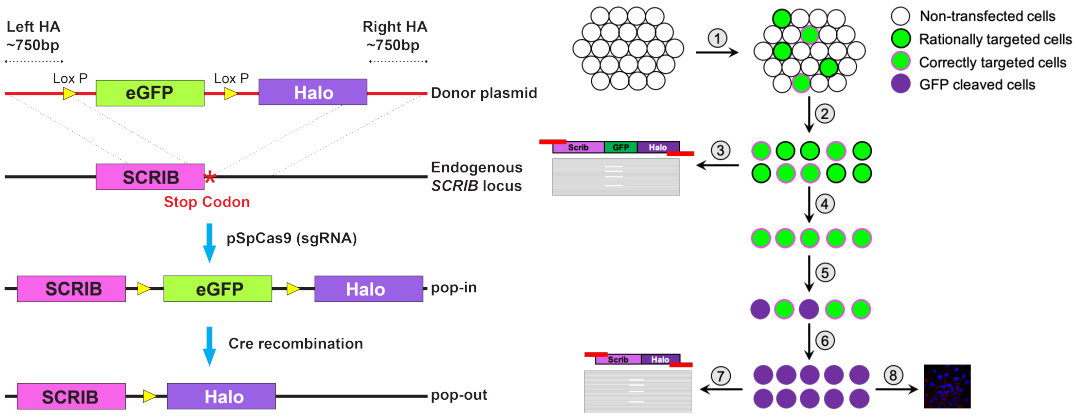

Figure 2.1 A two-step CRISPR/Cas9 genome editing strategy for in-frame HaloTag fusion in MDCK cells.

The workflow to generate this cell line includes 8 steps: (1) Co-transfection of Cas9/sgRNA and DT plasmids; (2) Fluorescence-activated cell sorting (FACS) to collect GFP positive cells; (3) PCR screen for clones that underwent HDR; (4) Single cell clone isolation; (5) Introducing plasmids encoding Cre enzyme into cell clones that underwent HDR; (6) Fluorescence-activated cell sorting (FACS) to collect GFP negative cells; (8) Cellular imaging and gel analysis.

The PCR screen results demonstrate that only one of the two alleles of SCRIB undergone HDR in all the CRISPR edited clones (**Figure 2.2A-B**). Expression of Scribble-HaloTag fusion protein was detected using Janelia Fluor™ 646 (**Figure 2.2C**) (Grimm et al., 2017).

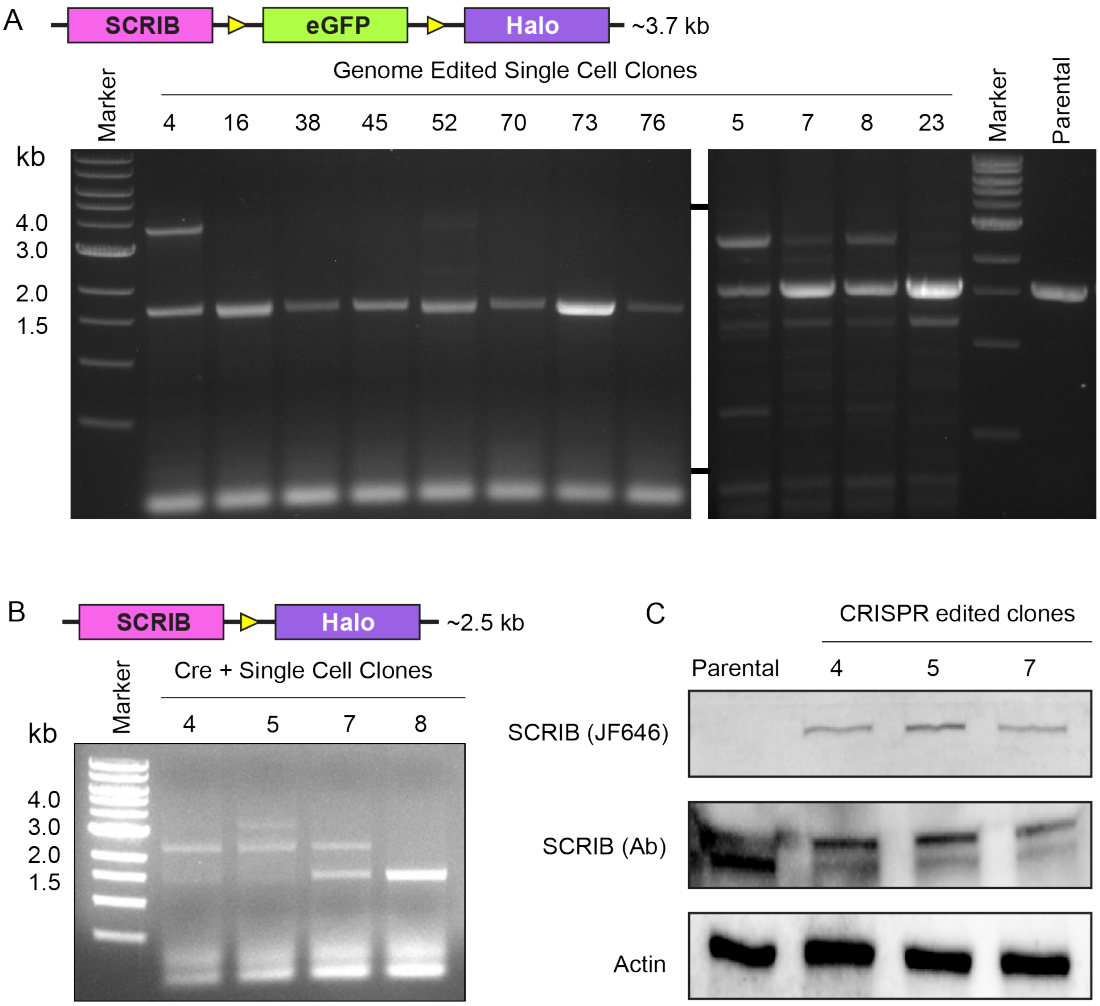

Figure 2.2 PCR screen for clones that underwent HDR.

(A) PCR products from genomic DNA of the GFP-positive MDCK single cell clones and untreated parental cells, were visualized by gel electrophoresis. Among the 12 clones shown, 4 generated PCR products of the expected size (~3700bp). (B) PCR screen for clones in which the GFP expression cassette was removed through Cre recombination. PCR products amplified from genomic DNA of the original GFP-positive clone after Cre recombination were visualized by gel electrophoresis. After the GFP expression cassette is removed by Cre recombination, the size of the PCR product decreases to ~2500bp. (C) Western blot

of lysates of parental MDCK cells and edited clones expressing Scribble-Flag-HaloTag using JF 646 HaloTag ligand or anti-Scribble antibody.

Labeling Scribble-HaloTag with JF646 (**Figure 2.3A**) in confocal microscopes demonstrate that HaloTag knock-in does not affect Scribble membrane targeting and tight junction localization (**Figure 2.3B**).

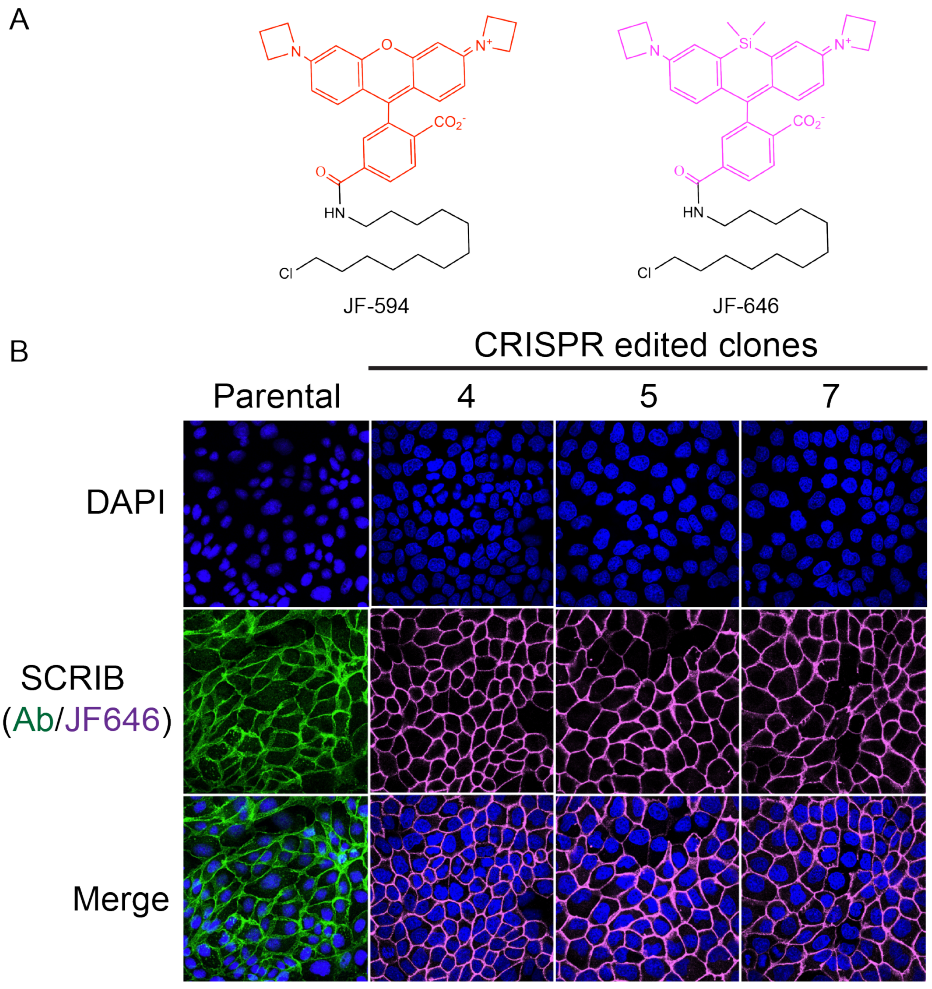

Figure 2.3 Labeling Scribble-HaloTag with JF646.

(A) Chemical structure of JF 646 and JF 594 HaloTag ligands used in this study. (B) Confocal microscopies of parental MDCK cells and edited clones expressing Scribble-Flag-HaloTag using JF 646 HaloTag ligand or anti-Scribble antibody.

We next displaced Scribble from tight junction by introducing Tet-On Systems for doxycycline-inducible Snail-T2A-GFP expression cassette (**Figure 2.4**) into cells as Snail overexpression disrupted tight junction (Ikenouchi et al., 2003).

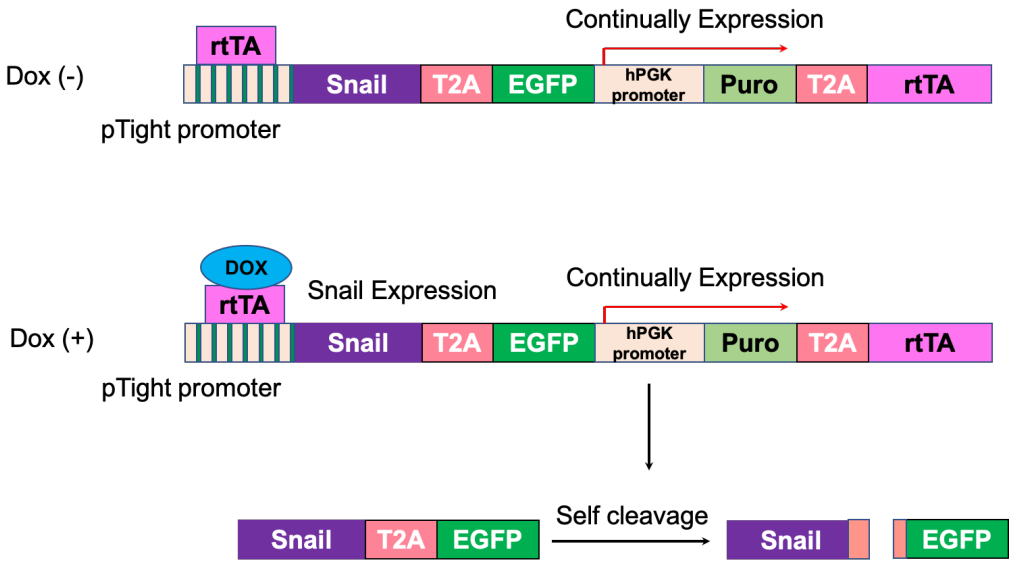

Figure 2.4 Schematic of Tet-On systems for Snail-T2A-GFP expression construct.

As expected, Snail expression induced cell morphological changes (**Figure 2.5**) as no tight junctions are formed. Moreover, Scribble demonstrates completely different patterns of subcellular localization (**Figure 2.5**). Removing doxycycline did not rescue this phenotype, suggesting that the alterations induced by Snail overexpression is irreversible. Overall, we successfully built a cell model in which Scribble is dysregulated, mimicking its status in malignant cancer cells.

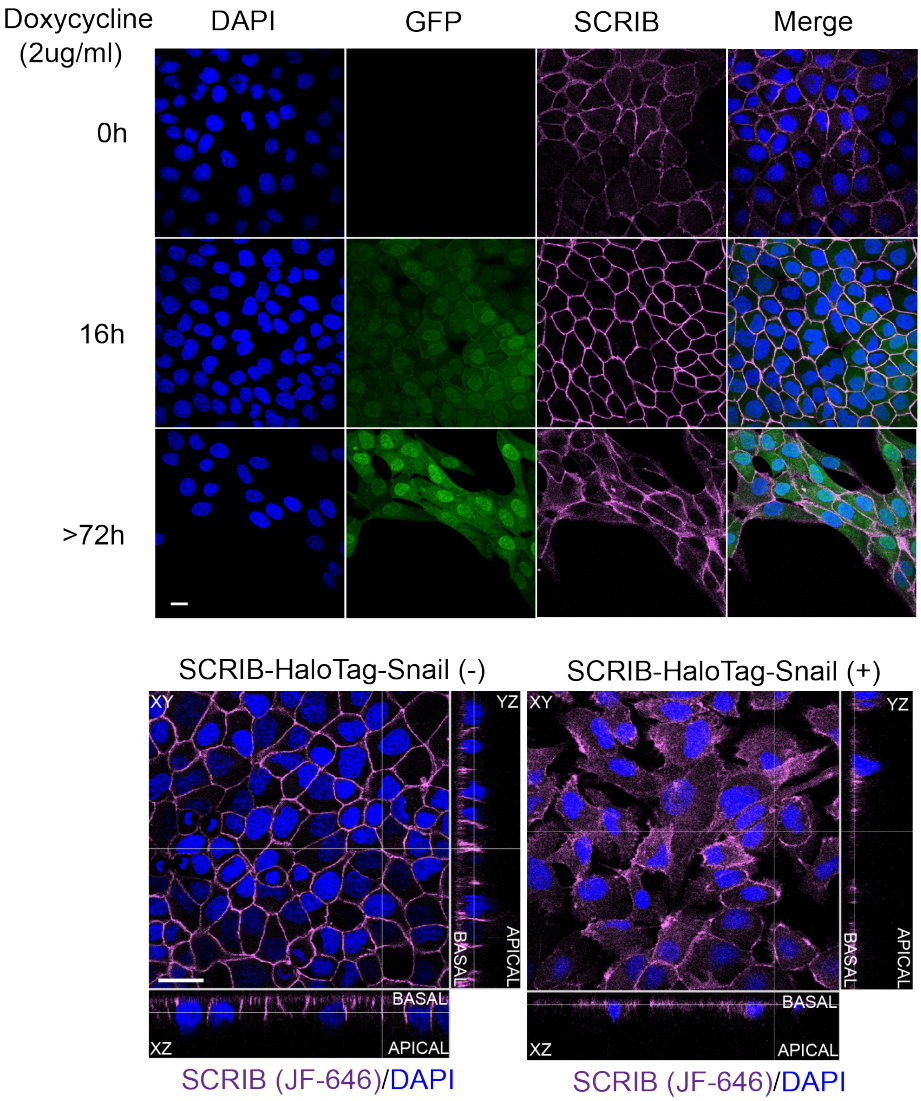

Figure 2.5 Doxycycline induced Snail expression disrupted cell polarity and Scribble subcellular localization.

Cellular localization of Scribble and cell morphology changes were analyzed at different time point in the presence of 2 μg/ml doxycycline.

As one of the hallmarks of cancer, aberrant YAP nuclear accumulation and activation has been observed in numerous cancers (Zanconato et al., 2016). Compared with its normal counterpart, our cancerous cell line model shown enhanced YAP nuclear localization (**Figure 2.8A**). Since Scribble has been reported to regulate YAP-S127 phosphorylation (Xu et al., 2018),

our first thought dephosphorylation YAP at serine 127 leads to its nuclear localization (**Figure 2.6**).

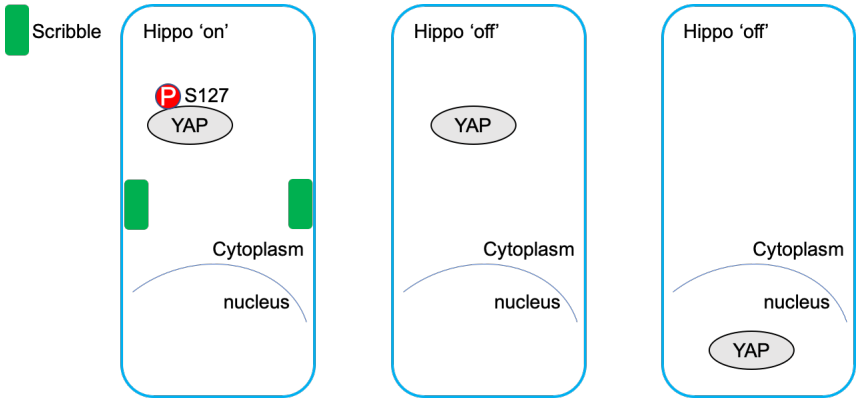

Figure 2.6 YAP phosphorylation at Serine 127 is reduced when Hippo signaling is off.

Surprisingly, YAP-S127 phosphorylation level is unchanged (**Figure 2.8B**). Instead, we detected elevated YAP phosphorylation at tyrosine 357 (**Figure 2.8B**), an alternative mechanism to facilitate YAP nuclear translocation and beta-catenin interaction to drive oncogenic Wnt signaling pathway (Rosenbluh et al., 2012), implying that Scribble may also play a role in YAP-Y357 phosphorylation (**Figure 2.7**).

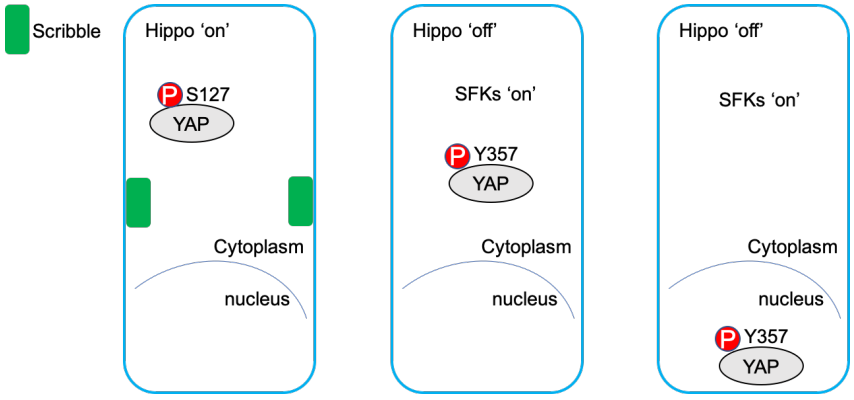

Figure 2.7 Src family kinase mediates YAP-Y357 phosphorylation and subsequent nuclear localization in beta-catenin driven cancer cells.

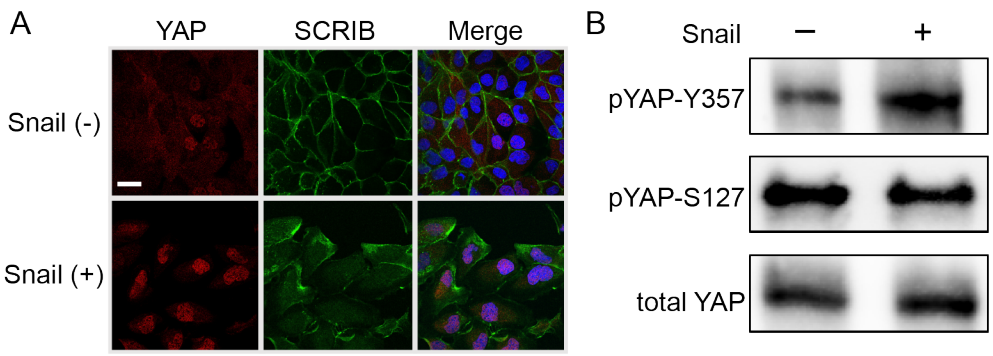

Figure 2.8 YAP phosphorylation at tyrosine 357 is elevated in Snail transformed cells.

(A) YAP demonstrate aberrant nuclear localization in MDCK-Scribble-HaloTag-Snail (+) cells. (B) Western blot analysis reveals a significantly up-regulated p-YAP-Y357 levels in MDCK-Scribble-HaloTag-Snail (+) cells, while p-YAP-S127 level is unchanged.

To determine whether YAP Y357 phosphorylation is a direct consequence of Scribble dysregulation, or is due to Snail induced pleiotropic effects, we used HaloPROTAC degrader to knockdown Scribble in our engineered cells (Buckley et al., 2015). Consistent with our hypothesis, knockdown of Scribble in Snail transformed cells attenuated YAP-Y357 phosphorylation, indicating that Scribble is involved in the regulation of YAP-Y357 phosphorylation (**Figure 2.9**).

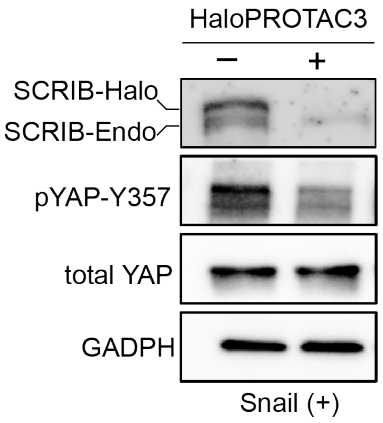

Figure 2.9 HaloPROTAC-mediated degradation of Scribble-HaloTag fusion proteins.

MDCK-Scribble-HaloTag-Snail (+) cells were treated with 1 μM HaloPROTAC3 for 16 hours. Scribble, YES1, p-YAP-Y357 and total YAP levels were measured by Immunoblot analysis.

Considering Scribble itself is a multi-domain scaffolding protein and has no tyrosine kinase activity, we suspected that Scribble mediated YAP-Y357 phosphorylation via a member of tyrosine protein kinase. To date, there are 58 receptor tyrosine kinases and 32 non-receptor protein kinases identified in human (Robinson et al., 2000), among which Abl and Src kinase family members have been reported to phosphorylate YAP at tyrosine 357 (Keshet et al., 2015; Levy et al., 2008; Rosenbluh et al., 2012; Sugihara et al., 2018; Sun et al., 2018; Tamm et al., 2011).

To identify the potential Scribble interacting tyrosine kinases at endogenous levels, we performed multiplexed, quantitative AP-MS analysis in our cell model. The design of our proteomic experiment is described in detail in **Methods**. Briefly, to perform a 'clean' MS, all samples for each replicate were incubated with: JF-594 for negative control sample; or DMSO for experimental sample. Such negative controls prevent Scribble-HaloTag binding to the beads.

Scrib-complexes were extracted using HaloTag beads, followed by in-gel digestion (**Figure 2.10**).

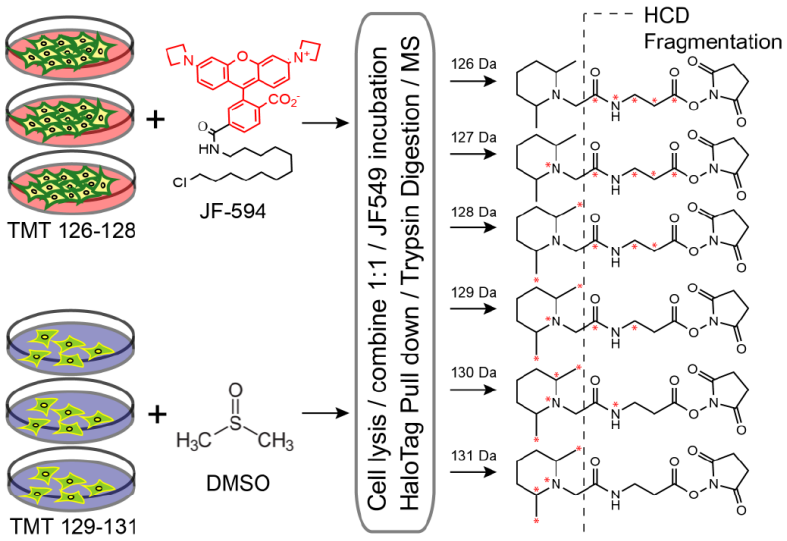

Figure 2.10 Design of proteomic experiment.

MDCK-Scribble-HaloTag-Snail (+) cells were incubated with either JF-594 or DMSO, then lysed. Protein complexes were enriched with HaloTag beads, then eluted and digested. Resulting peptides were chemically labeled with the indicated TMT labels. Samples were then combined as shown and analyzed by liquid chromatography and tandem MS.

Blocking and Pull-down efficiency were confirmed before further analysis (**Figure 2.11**). Cell lysates from negative control group (treated with JF-594) and experimental sample group (treated with DMSO) were incubated with JF-646 before and after incubation with HaloTag beads for 30min at room temperature. Blocking and pull-down efficiency were analyzed by detecting HaloTag ligands signal in Cy3 or Cy5 channel.

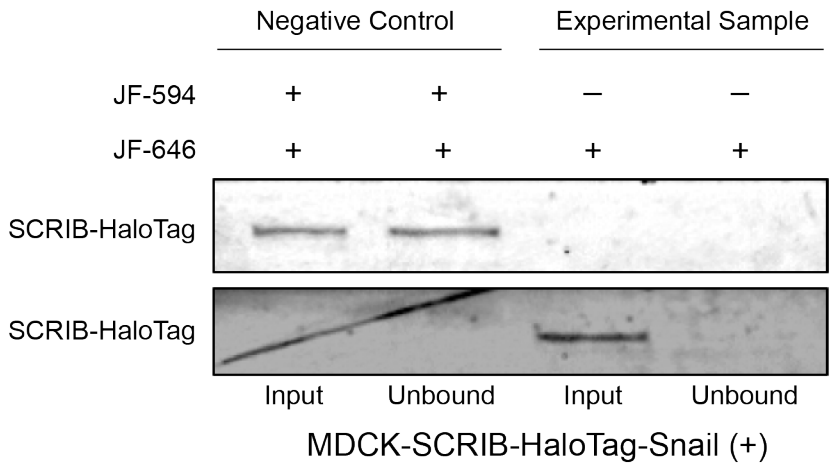

Figure 2.11 Blocking and pull-down efficiency were analyzed by detecting HaloTag ligands signal in Cy3 or Cy5 channel.

Digested peptides were then chemically tagged with MS-differentiable tandem mass tagging (TMT) labels. Thereafter the six samples were pooled and analyzed as a mixture by liquid chromatography-tandem MS, and raw data were analyzed by MaxQuant. We used stringent criteria, only proteins that were identified in all three replicates were continued for further analysis. Possible Scribble-interacting proteins were selected based on the following criteria: (1) a ratio of -JF594/+JF594 $\geqslant$ 1.70 and (2) a p value $\leqslant$ 0.05 (-JF594/+JF594). After such rigorous screen, only 6 proteins meet both criteria, including non-receptor protein kinase YES1 (**Figure 2.12**). Several previously identified Scribble-interacting proteins, such as Vimentin, beta-catenin, ZO-1, beta-spectrin, and Plakophilin 4 were also identified. However, except for Vimenin, other proteins did not meet our criteria described above. This might result from the low abundance of these proteins or because of our endogenous MS. Meanwhile, since Vimentin is overexpressed while YES1 is not, the MS results indicate that Scribble-YES1 might be a prime interaction in our Snail transformed cell model.

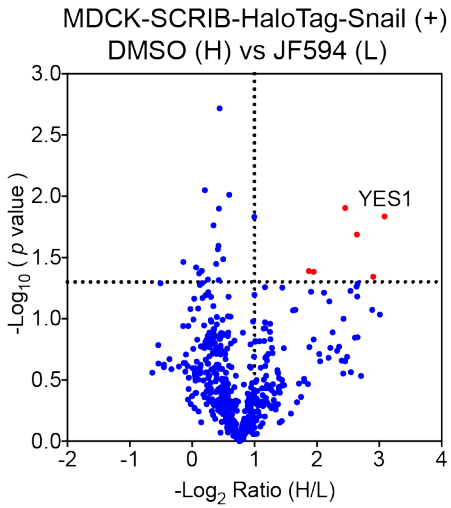

Figure 2.12 Volcano plot of -JF594/+JF594 enrichment for YES1.

Proteins meeting the criteria of a p value ≤ 0.05 and ratio ≥ 1.70 were assigned as putative Scribble interactors, which were marked as red.

To investigate our MS results, Scribble and YES1 were co-expressed in HEK 293T cells, a canonical host to transient express exogenous protein and tight-junction free cell line (Cording et al., 2013), and their interaction can be validated in vivo (**Figure 2.13**).

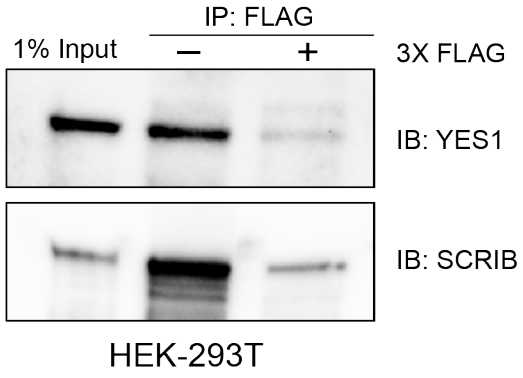

Figure 2.13 Co-IP of Scribble with YES1 in HEK-293T cells.

FLAG-immune complexes were isolated from cells and analyzed by Immunoblot with anti-Scribble and anti-YES1 antibody. As a negative control, 2 µL of 25 µg/µL 3X Flag peptide were added into cell lysates.

Their co-localization can also be observed in our engineered cell lines. Although Scribble and YES1 co-localize in both normal and Snail-expressing cells, their overall distribution is dramatically altered. In normal cells, Scribble and YES1 uniformly localize at cell-cell junctions. In both Snail-expressing MDCK cells and human MDA-MB-231 cells, both Scribble and YES1 co-localize as small puncta distributed across all membranes and cytoplasm. (**Figure 2.14**).

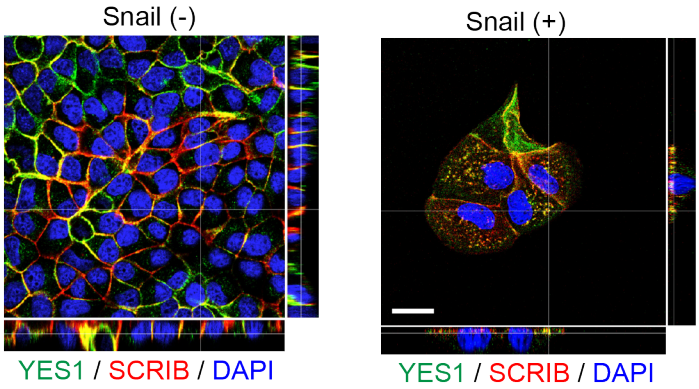

Figure 2.14 Co-localization of Scribble with YES1 in MDCK-Scribble-HaloTag-Snail (+) / (-) cells.

Cells were fixed in PFA and processed for double fluorescence by using JF 646 and mouse anti-YES1 antibody. Confocal fluorescence microscopy showed the co-localization of Scribble and YES1 in superimposed images.

Surprisingly, although Scribble and YES1 demonstrated co-localization in both cell lines, we could only detect Scribble-YES1 interaction in the cancerous cell line (**Figure 2.15**). Accordingly, other studies reported that YES1 form a stable complex with occludin while Scribble participates in the Scribble/Dlg/Lgl polarity module at cell-cell junction, respectively (Chen et al., 2002; Humbert et al., 2008). Moreover, overexpression of Snail repressed the gene expression of occludin (Ikenouchi et al., 2003), thus YES1 is likely liberated from occludin complex in our cancerous cell line. Therefore, we reasoned that Scribble can only form a complex with YES1 when the tight junction is disrupted, in which they are both released from their original Protein-Protein Interaction complexes (PPIs).

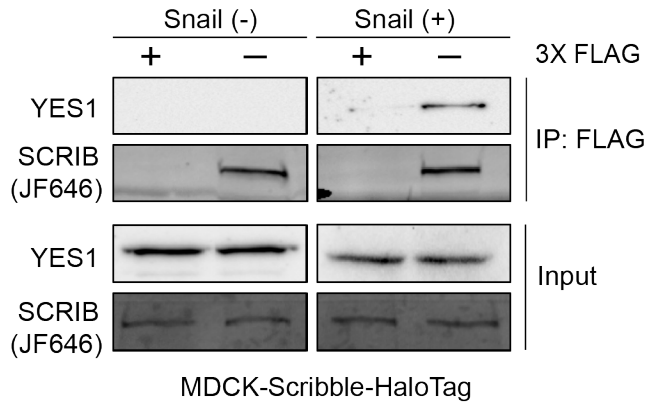

Figure 2.15 Co-IP of Scribble with YES1 in MDCK-Scribble-HaloTag-Snail (+) / (-) cells.

FLAG-immune complexes were isolated from cells and analyzed by Immunoblot with JF 646 and anti-YES1 antibody. As a negative control, 2 µL of 25 µg/µL 3X Flag peptide were added into cell lysates.

We further validated Scribble-YES1 interaction in MDA-MB-231 cells (**Figure 2.16**). We choose MDA-MB-231 cells for three reasons: Snail is highly expressed (Aigner et al., 2007), Scribble is dysregulated (Zhan et al., 2008) and YES1 is activated (Meric et al., 2002). Interestingly, it has been reported that YAP-Y357 phosphorylation is mediated by YES1 in beta-catenin active cancer cells (Rosenbluh et al., 2012).

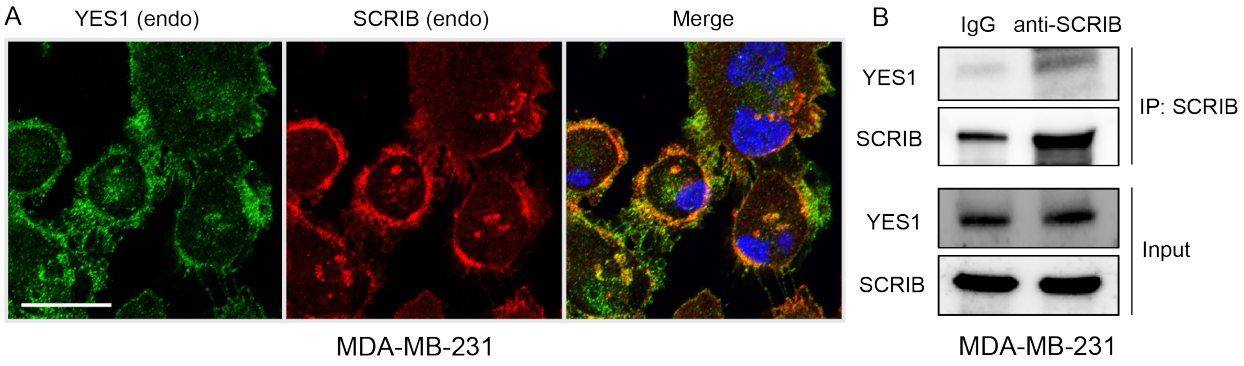

Figure 2.16 Co-localization and co-immunoprecipitation of Scribble with YES1 in MDA-MB-231 cells.

Cells were fixed in PFA and processed for double fluorescence by using goat anti-Scribble and mouse anti-YES1 antibodies. Confocal fluorescence microscopy showed the co-localization of Scribble and YES1 in superimposed images in MDA-MB-231

cells. For immunoprecipitation in MDA-MB-231 cells, lysates were incubated with the antibody/bead complex for 4 hours at 4°C. Beads were washed with the 1X TBS containing 0.005% and then re-suspended in 2X SDS loading buffer.

We also observed activation and accumulation of nuclear beta-catenin in our cancerous cells (**Figure 2.17**), suggesting that to some extent, our genetically induced cancer model mimics beta-catenin driven cancer cells. Overall, these studies validate the bona fide Scribble and YES1 interaction. Using our combined chemical biology strategy, for the first time we discovered that Scribble and YES1 are involved in the same protein complexes and in the overlapping YAP-Y357 phosphorylation signaling cascades.

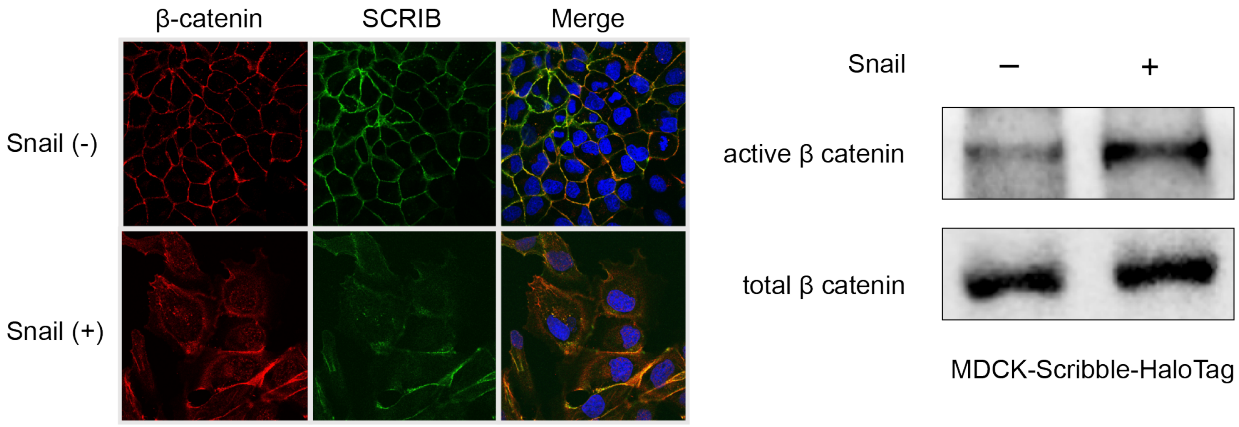

Figure 2.17 Beta-catenin is activated in MDCK-Scribble-HaloTag-Snail (+) cells.

(A) Beta-catenin demonstrate aberrant nuclear localization in MDCK-Scribble-HaloTag-Snail (+) cells. (B) Western blot analysis reveals beta-catenin is activated in MDCK-Scribble-HaloTag-Snail (+) cells.

As mentioned above, active YES1 adopts an open configuration, whereas inactive YES1 is characterized by a closed and compact structure stabilized by inhibitory intramolecular interactions. Thus, we next sought to investigate whether Scribble interacts with active or inactive YES1 using conformation-selective inhibitors targeting kinase domain of SFKs

(Kwarcinski et al., 2016). For instance, both Dasatinib and SKI-1 inhibits Src kinase activity, however, Dasatinib induces Src kinase to adopt its active, open configuration, whereas SKI-1 induces Src kinase to adopts its inactive, close configuration (Koudelkova et al., 2019). Therefore, these inhibitors provide valuable chemical tools to study if Scribble interacts with active (open) or inactive (closed) YES1 as they can lock YES1 in a specific configuration despite the kinase activity. The inhibitors used in this study and their effect on SFKs structure were summarized in **Figure 2.18**.

Structure	Inhibitor	Binding mode	αC Helix orientation	Effect on SFKs Structure
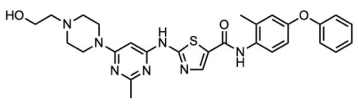	DAS-CHO-II	DFG-out	αC-out	Close
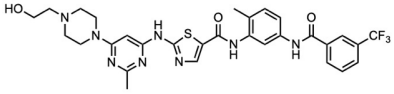	DAS-DFGO-II	DFG-out	αC-in	Open
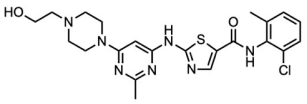	Dasatinib	DFG-in	αC-in	Open

Figure 2.18 Structures and Binding Modes of SFKs Inhibitors.

We choose HEK-293T as our expression system for two reasons: 1, Scribble and YES1 interaction in this cell line has been validated in this cell line; 2, YES1 is mainly inactive and adopts closed configuration in this cell line (Rosenbluh et al., 2012). Hence, the impact of altered YES1 configuration on Scribble-YES1 interaction can be readily compared before and after SFKs inhibitors treatment. Wild, membrane associated Scribble or cytoplasm localized Scribble-P305L mutant was co-transfected with YES1 in HEK 293T cells for 48h, then incubated with DMSO or respective inhibitors for 1h. Surprisingly, the inhibitors demonstrated opposing effects

on membrane associated Scribble and cytosolic Scribble-P305L mutant when compared with their corresponding DMSO treated positive controls.

In cells expressing membrane associated Scribble (WT), reduced YES1 interaction was observed in groups treated with Dasatinib and DAS-DFGO-II, which induce opening of YES1 structure, while close configuration inducible inhibitor DAS-CHO-II treatment enhanced interaction between Scribble and YES1 (**Figure 2.19**).

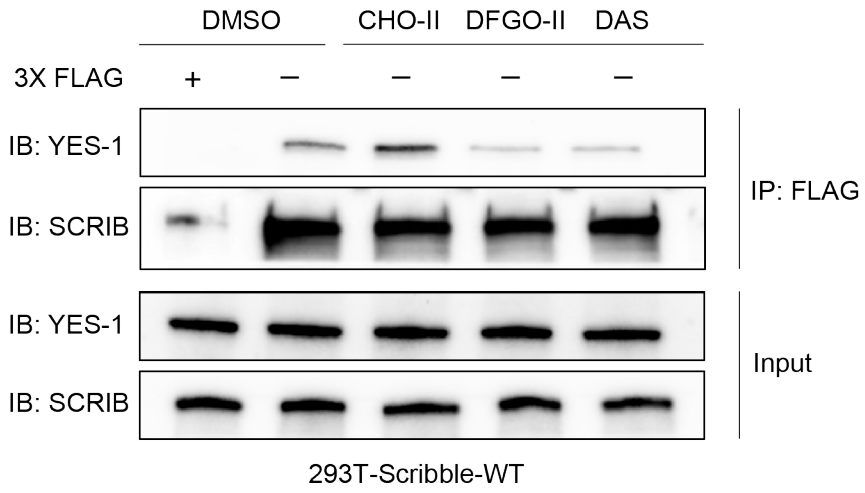

Figure 2.19 The impact of SFKs inhibitors on the interaction of wild type, membrane associated Scribble and YES1. HEK-293T cells expressing wild type Scribble-GFP-Flag and YES1 were incubated for 1h with 100nM SFKs inhibitors before cell lysis. FLAG-immune complexes were isolated from cells and analyzed by Immunoblot with anti-GFP and anti-YES1 antibody. As a negative control, 2 µL of 25 µg/µL 3X Flag peptide were added into cell lysates.

However, the effects were totally reversed in cells expressing cytosolic Scribble-P305L mutant (**Figure 2.20**). For cytosolic Scribble, no YES1 interaction was observed in groups treated with DAS-CHO-II, which induces closed configuration of YES1, while open configuration inducible inhibitor Dasatinib and DAS-DFGO-II treatment did not affect interaction between Scribble and YES1.

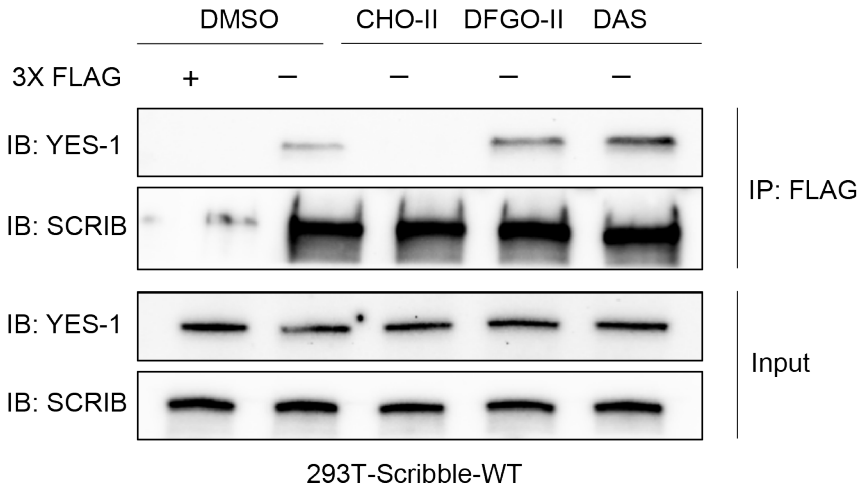

Figure 2.20 The impact of SFKs inhibitors on the interaction of P305L mutant, cytosolic Scribble and YES1.

HEK-293T cells expressing P305L mutant, cytosolic Scribble-GFP-Flag and YES1 were incubated for 1h with 100nM SFKs inhibitors before cell lysis. FLAG-immune complexes were isolated from cells and analyzed by Immunoblot with anti-GFP and anti-YES1 antibody. As a negative control, 2 μL of 25 μg/μL 3X Flag peptide were added into cell lysates.

Interestingly, we did not observe similar effects when we treat cell lysates with Src kinase inhibitors in vitro (**Figure 2.21**), implying that subsequent cellular events are required to accommodate YES1 configuration transition.

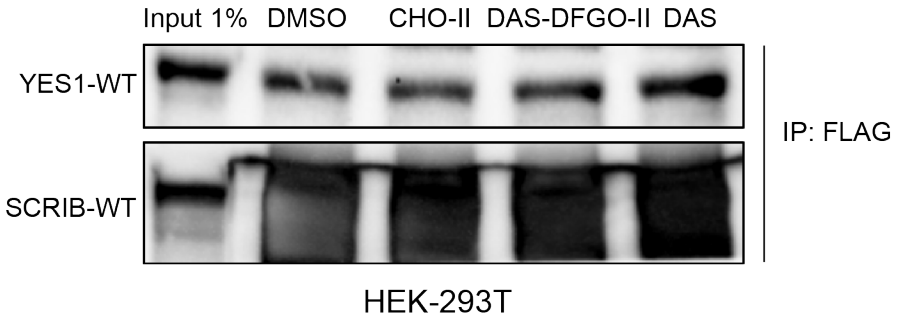

Figure 2.21 Treatment of HEK-293T cells expressing Scribble-WT and WT-YES1-GFP with SFKs inhibitors in vitro.

Cell lysates were equally divided and incubated with either DMSO or 500nM corresponding inhibitors for 30min at room temperature, then incubated with 50 μL Anti-FLAG M2 Magnetic Bead slurry overnight at 4°C.

Based on these results, we hypothesized that YES1 adopts different configurations to interact with membrane associated and cytosolic Scribble. Since YES1 is mainly inactive and adopts closed configuration HEK-293T cells (Rosenbluh et al., 2012). To test our hypothesis, we co-expressed YES1 with wild type Scribble or cytosolic Scribble-P305L mutant in this cell line. Consistent with our prior results, membrane associated Scribble preferably interact with close, inactive YES1, (**Figure 2.22**), while cytosolic Scribble seems only to interact with open, active YES1.

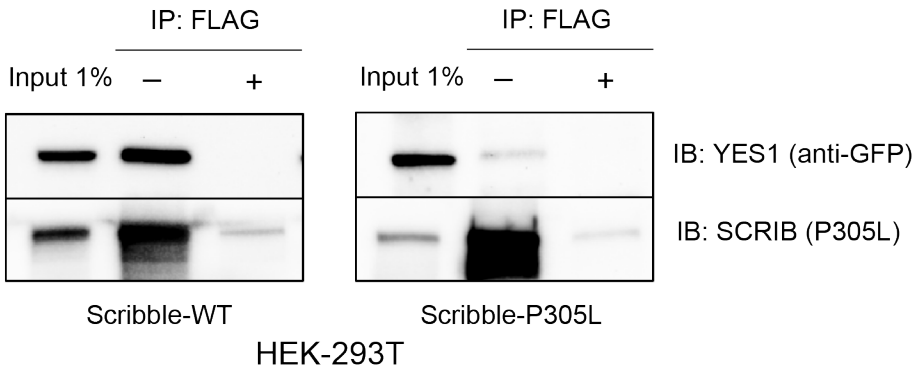

Figure 2.22 Interactions of Scribble-WT and P305L mutant with wild type YES1 in HEK-293T cells.

FLAG-immune complexes were isolated from cells and analyzed by Immunoblot with anti-Scribble and anti-GFP antibody. As a negative control, 2 µL of 25 µg/µL 3X Flag peptide were added into cell lysates.

To further confirm the effect of YES1 configuration on the Scribble-YES1 interaction and validate our hypothesis, we generated YES1 mutants which only adopt open or close configuration by introducing mutations Y537F and Q538E, P539E, G540I respectively (Schindler et al., 1999). Consistent with our prior results, membrane associated Scribble preferably interact with close, inactive YES1, (**Figure 2.23A**), while cytosolic Scribble can only interact with open, active YES1 (**Figure 2.23B**). Although Scribble-YES1 interaction can also be detected in (Scribble-WT, active YES1) group (**Figure 2.22**), the result is not in contradiction

with our conclusion as transient overexpressed Scribble is localized both in the membrane and cytoplasm in 293T cells (Okajima et al., 2008). Similarly, although transient expressed YES1 is mainly inactive, a fraction of YES1 is still active and adopts open configuration in 293T cells. Thus, a weak band of YES1 was observed in (Scribble-P305L, YES1-WT) group (**Figure 2.22**). Overall, these studies revealed that membrane associated Scribble preferably interacts with inactive YES1, while cytosolic Scribble only interacts with active YES1.

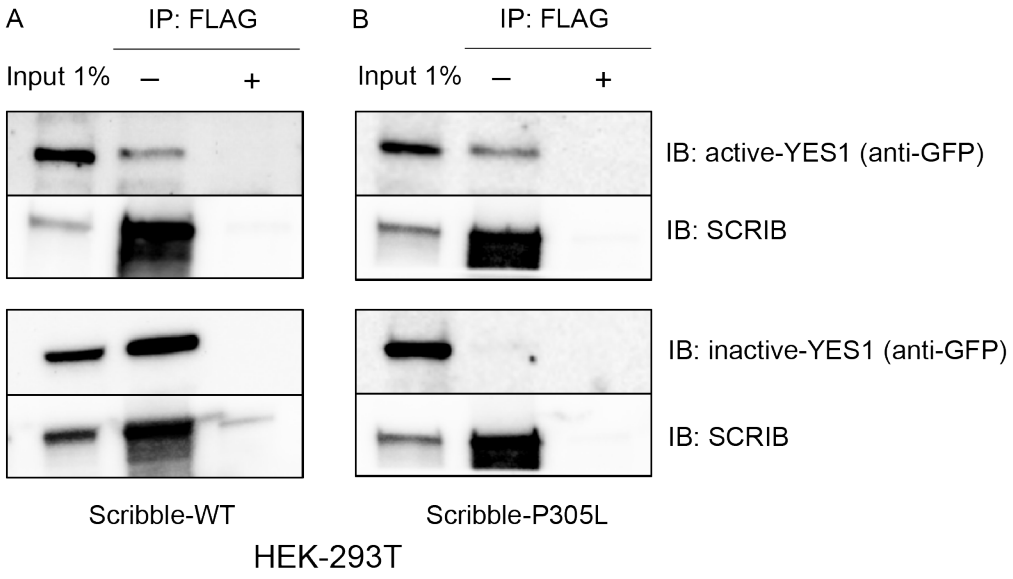

Figure 2.23 The interaction of Scribble and YES1 is dependent on Scribble localization and YES1 conformation.

FLAG-immune complexes were isolated from cells and analyzed by Immunoblot with anti-Scribble and anti-GFP antibody. As a negative control, 2 μL of 25 μg/μL 3X Flag peptide were added into cell lysates. (A) Interactions of Scribble-WT with active-YES1 or inactive-YES1. (B) Interactions of cytosolic Scribble-P305L mutant with active-YES1 or inactive-YES1.

As a scaffold protein, Scribble has been reported to protect its interacting partners from degradation and dephosphorylation (Michaelis et al., 2013; Young et al., 2013). Therefore, we firstly hypothesized that Scribble may prevent YES1 from degradation to regulate YAP-Y357 phosphorylation. Despite reduced YAP-357 phosphorylation was observed, siRNA knockdown of Scribble shown no effects on YES1 at protein levels in MDA-MB-231 cells, and vice versa

(**Figure 2.24A**). Note that total YAP levels were unchanged post 24h of Scribble or YES1 knockdown, while significantly reduced after 48h (**Figure 2.24B**). This phenomenon is consistent with the fact that phosphorylation of YAP at tyrosine 357 is related to YAP stability (Levy et al., 2008).

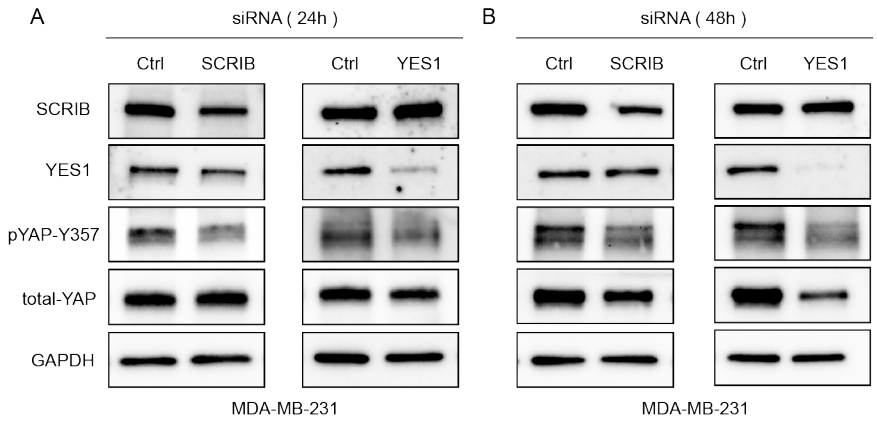

Figure 2.24 siRNA knockdown of Scribble and YES1 in MDA-MB-231 cells.

(A) MDA-MB-231 cells were incubated with Scribble or YES1 siRNA for 24 hours. (B) MDA-MB-231 cells were incubated with Scribble or YES1 siRNA for 48 hours. Total YPA and YAP phosphorylation on Try 357 were analyzed by Immunoblot with anti-YAP and anti-YAP-Y357 phosphorylation antibody, respectively.

We next hypothesized that Scribble and YES1 interaction affects YES1 activation. Usually, to investigate if a certain biological effect is caused by a specific PPI, the interaction domains should be mapped first, then the impact of this PPI on the biological function can be measured by disruption of PPI via domain mutation or truncation. However, the unique Scribble-YES1 interaction provides a shortcut to address this question as cytosolic Scribble has no interaction with inactive YES1. Therefore, we co-expressed membrane associated Scribble and cytosolic Scribble-P305L mutant with wild type YES1 in 293T cells, and compared the phosphorylation levels of YES1 at tyrosine 426, a marker of YES1 activation (Boczek et al., 2019). We found that wild type Scribble expression significantly increased YES1 Y426

phosphorylation when compared with YES1 expression alone. Meanwhile, expression of Scribble-P305L mutant did not affect YES1 Y426 phosphorylation (**Figure 2.25A-B**). Therefore, we concluded that membrane associated, but tight junction excluded Scribble interacts with YES1 and facilitates its activation, suggesting that Scribble tight junction localization is required for its tumor-suppressive function. However, the function of cytosolic Scribble and active YES1 interaction is still unknown.

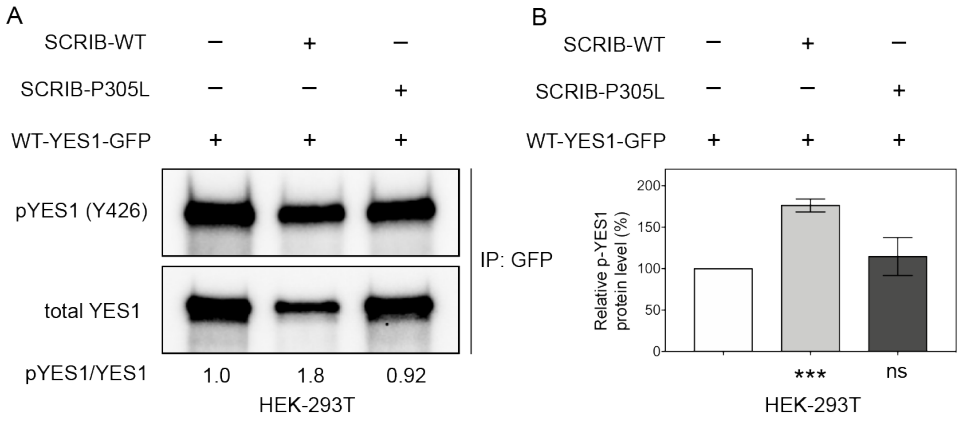

Figure 2.25 Membrane associated Scribble interacts with YES1 and promotes YES1 activation.

(A) Wild type YES1 was co-transfected with empty vector, Scribble-WT or Scribble-P305L plasmids. After 48 hours, WT-YES1-GFP was isolated with GFP-Trap Resin and phosphorylation levels of YES1 at tyrosine 426 was analyzed by Immunoblot using anti-Phospho-Src Family (Y416) antibody. (B) Western blot analysis reveals significantly up-regulated pYES1-Y426 in cells expressing Scribble-WT. The ratio of pYES1-Y426 to total YES1 was quantified and normalized to the YES1 expression alone group. Means ± SEM of n = 3 independent experiments are indicated. Student's t-test; ***P < 0.001.

Discussion

In this study, we identified and characterized the molecular basis of Scribble and YES1 interaction. In particular, we found that Scribble and YES1 interaction is dual-controlled by Scribble localization and YES1 conformation. However, whether their interaction is direct or

indirect is unclear. Although YES1 contains PDZ binding motif on its very C terminus (Radziwill et al., 2007), this motif belongs to the type III PDZ binding motif thus it is not recognized by the PDZ domains of Scribble (Ivarsson et al., 2014). Also, it is unlikely that Scribble is a substrate of YES1 and thus to activate YES1, as no SH3-binding motif can be found in Scribble sequence. Therefore, we reasoned that Scribble interacts with YES1 in an indirect way.

Another mechanism of YES1 activation is mediated through upstream phosphatases (Sen and Johnson, 2011). Interestingly, a few protein tyrosine phosphatases were enriched in the potential Scribble interacting complexes in our AP-MS, including PTPN13, PTP-PEST, among which PTPN13 has been reported to repress Src kinase activity (Glondu-Lassis et al., 2010) while PTP-PEST to activate Src kinase activity (Chellaiah and Schaller, 2009). If Scribble and YES1 interaction is bridged by these phosphatases, the net results of Scribble and YES1 interaction will be determined by a balance among such phosphatases. We also found that cytosolic Scribble interacts only with active YES1. As a scaffold protein, Scribble may function as a reactive center facilitating YES1 substrate recognition. However, further investigation is still required to validate this hypothesis and figure out the function of such interaction. Finally, a lesson should be learned from the story of Scribble-YES1 interaction: when exploring protein-protein interaction, expression system must be carefully selected as protein localization and conformation may be varied among different cells.

Materials and Methods

Mammalian Cell Culture

HEK-293T, parental or CRISPR-Cas9 mediated MDCK, and MDA-MB-231 cells from the ATCC (passages <25) were cultured in DMEM (Thermo Fisher Scientific) supplemented with 10% fetal bovine serum at 37°C under 5% CO2. Mycoplasma testing was not performed before experiments. For the fluorescence microscopy imaging experiments, cells were grown on 8-well Nunc LabTM-TekTM II chamber slides.

CRISPR/Cas9 Guide and Donor Plasmid Construction.

Guide RNA construction was performed as described previously in the detailed protocol (Ran et al., 2013). Briefly, two guide sequences, sgRNA1: TGGGCCCCGTGCCCTCCTAG and sgRNA2: GGGGAGGTTCTGGAGCCTCT targeting the C-terminal region of SCRIB were designed and ligated as complementary oligonucleotides into the pX330-U6-Chimeric_BB-CBh-hSpCas9 (PX330) expression construct (Addgene plasmid # 42230) linearized by the restriction enzyme BbsI.

Homology arms with the endogenous SCRIB sequence, left (NC_006595.3, chr13: 37373794-37374526) and right (NC_006595.3, chr13: 37374527-37337528) were PCR amplified from MDCK genomic DNA. HaloTag sequences and the FLAG-loxP-EGFP-loxP expression cassette were PCR amplified from pH6HTN His6HaloTag® T7 Vector (Promega # G7971) and pUC57-FLAG-LoxP-GFP-LoxP-SNAP-TERT expression construct (Addgene plasmid # 71391), respectively. These PCR fragments were assembled with In-Fusion HD Cloning Plus Kits (Takara # 638909). All the sequences of the primers used in this study are listed in the Table 2.

Establishment of MDCK Cell Lines with HaloTag Knock-in at the C Terminus of Endogenous SCRIB

The overall strategy has been described in detail elsewhere (Xi et al., 2015). Briefly, MDCK cells in 6-well plate were transfected at ~ 60%–70% confluency with the CRISPR-Cas9 vector pX330 containing the sgRNA (1,000 ng) and the donor plasmid (1,000 ng) using Lipofectamine™ LTX Reagent with PLUS™ Reagent according to the manufacturers' instructions. After 14 days, cells that underwent homologous recombination with the donor plasmid were screened for GFP signal and confirmed by PCR. Next, the GFP expression cassette was removed from the SCRIB locus through Cre-mediated recombination. GPF negative cells were collected as single cell clones and confirmed by PCR. To establish a Tet-On Systems for doxycycline-inducible Snail expression in MDCK-SCRIB-HaloTag cells, Snail-T2A-GFP expression cassette was built and In-Fusion cloned into pCW57.1-Cas9 vector (Addgene # 50661) in which Cas9 was cleaved with NheI and BamHI. The doxycycline-inducible Snail vector was introduced into cells via lentivirus transduction. Then cells were selected with 4ug/ml puromycin for 2 weeks and screened for strong GFP signal in the presence of 2ug/ml doxycycline.

Virus Production and Transduction.

For preparation of lentiviruses or retroviruses, HEK 293T cells in 60-mm dish were transfected at ~ 90% confluency with the lentiviral vector containing the gene of interest (4,000 ng), the lentiviral packaging plasmids psPAX2 (3,000 ng) and pMD2.G (1,200 ng), or with the retroviral vector containing the gene of interest (4,000ng) and the pCL-Ampho Retrovirus Packaging Vector, plus 24μL of Fugene HD (Promega # E2311) for 8 hours, respectively. Media was

changed 24 hours after transfection. About 60 hours after transfection the cell medium containing lentivirus was harvested and filtered through a 0.45-μm filter. Target cells were then infected at ~ 50% confluency in media containing 8 μg/mL of polybrene, followed by selection with the appropriate antibiotics before further analysis.

Knockdown Experiment

To knockdown SCRIB in MDCK-SCRIB-HaloTag cells, cells were treated with 1 μM HaloPROTAC3 for 16 hours. SCRIB-HaloTag fusion protein degradation was confirmed by immunoblotting. For siRNA knockdown, MDA-MB-231 cells were seeded in 60-mm dish to reach the ~30% confluency at the day of transfection. 3ml complete medium was freshly added to the cells 60min before transfection. siRNA was diluted into 300μL of 1X PepMute™ Transfection Buffer to make the final concentration of 30 nM respectively per dish. 9μL of PepMute™ reagent was added and incubated for ~15 min at RT. The transfection mix was added into cells drop wise and gene silencing was measured 24 or 48 hours post transfection.

Labelling SCRIB-HaloTag Fusion Protein with Janelia Fluor™ Dyes

In this study, SCRIB-HaloTag fusion protein was labelled with either Janelia Fluor™ 594 (JF594) or Janelia Fluor™ 646 (JF646). For confocal experiments, HaloTag ligands were added to the growth medium to make the final concentration of 10nM and incubated MDCK-SCRIB-HaloTag cells for 15min. Cells were then washed briefly with complete culture medium and incubated in complete culture medium for an additional 15min. Next, cells were washed briefly with 1X PBS for a total of three times. Before imaging, cells were then fixed with 4% paraformaldehyde in PBS at room temperature for 20min, quenched and washed thoroughly with

1X TBS. To detect SCRIB-HaloTag fusion protein in gel-based analysis, 10 μL cell lysates were incubated with 1 μL HaloTag ligands at the concentration of 10uM at room temperature for 30min, then mixed with 10 μL 2X SDS loading buffer and boiled at 95°C for 5 minutes. After gel electrophoresis, HaloTag ligands signal was detected either in Cy3 or Cy5 channel.

Immunofluorescence Staining

Cells were seeded and grown for 24 hours. Subsequently, the cells were fixed with 4% paraformaldehyde for 20 min, permeabilized with 0.1% Triton X-100, blocked in 3% BSA in PBS. Cells were incubated with the designated primary antibodies (1:200) in 1% BSA overnight at 4°C, secondary antibodies (1:1000) in 1% BSA at room temperature for 1h, and extensively washed with PBS between each step. Fixed and stained samples were imaged using Nikon Eclipse Ti Confocal Microscope.

Site-Directed Mutagenesis

Mutagenesis of the YES1 was performed on the pEGFP-N1-YES1 plasmid (Addgene # 110497) by PCR-based site-directed mutagenesis using QuickChange II XL Site-Directed Mutagenesis Kit (Agilent # 200522). YES1-Y537F mutant was constructed by replacing TAC by TTC. YES1-Q538E, P539E, G540I triple mutant was constructed by replacing CAG by GAG, CCA by GAG, GGA by ATA, respectively. Mutated sequences were confirmed by Sanger sequencing.

Transfection, Cell Lysate Preparation and Immunoprecipitation

To immunoprecipitate SCRIB complexes from cell lysates, 5ug of the corresponding YES1-GFP constructs were co-transfected with either 5ug empty vector or FLAG-epitope tagged hSCRIB

mammalian expression vector into HEK 293T cells seeded in 60-mm dish at ~ 90% confluency using Lipofectamine 3000 reagent (Thermo ScientificTM, L3000008). After 24 hours, cells were trypsinized, re-plated into 100mm tissue culture dish and incubated at 37°C under 5% CO2 for an additional 24 hours. After 48 hours transfection, cells were briefly washed with cold 1X PBS, scraped from dish and centrifuged at 2,000g for 10min at 4°C.

For SFKs inhibitory experiments, cells were incubated with 100nM SFKs inhibitors for 1h at 37°C before cell lysis. The cell pellets were frozen at –80°C for at least 1h prior to be lysed in 1ml cold cell lysis buffer (0.05% NP-40, 50mM Tris-HCl (pH 7.0), 150mM NaCl) containing Protease Inhibitor Cocktail (Promega, G6521) and Halt™ Phosphatase Inhibitor Cocktail (Thermo ScientificTM, 78420). Cell lysates were passed through 27-gauge needle 10 times and centrifuged at 14,000g for 10min at 4°C to clear the lysate. 5 µL of cell lysates were taken out as input. Next, cell lysates were split into two parts, each for a volume of 500 µL plus 2 µL 1XTBS as the sample group while 2 µL of 25µg/µL 3X Flag peptide solution as the negative control group, respectively. Each group of cell lysates was mixed with 500 µL of 1X TBS containing 50 µL Anti-FLAG M2 Magnetic Bead slurry (Sigma Aldrich # M8823) overnight at 4°C, then washed gently with 1X TBS containing 0.005% NP-40 for a total of three times. The SCRIB complexes were eluted from the beads with 20 µL of 1% SDS in a shaking incubator for 30min at 37°C, then mixed with 10 µL 4X SDS loading buffer and boiled at 95°C for 5 minutes before gel electrophoresis. To immunoprecipitate YES1-GFP, cell lysates were incubated with 25 µL of GFP-Trap Resin (ChromoTek # gtma-10) for 1h at 4°C, washed extensively and directly boiled with 30 µL 1X SDS loading buffer for 5min. For immunoprecipitation in MDA-MB-231 cells, SureBeads™ Protein G Magnetic Beads (Biorad # 1614023) were incubated with the SCRIB antibody (Santa Cruz # sc-11049) at 4°C for 1 hour in lysis buffer plus 20 mg/ml BSA.

Subsequently, beads were washed with lysis buffer prior to adding cleared cell lysates. Lysates were incubated with the antibody/bead complex for 4 hours at 4°C. Beads were washed with the 1X TBS containing 0.005% and then re-suspended in 2X SDS loading buffer.

SCRIB-HaloTag Complexes Pull Down and MS Sample Preparation

MDCK-SCRIB-HaloTag-Snail (+) cells were pre-incubated with Janelia Fluor™ 594 (JF-594) or DMSO. Cells were then lysed in 1ml cold cell lysis buffer as described above, and mixed with 100μL of Magne® HaloTag® Beads (Promega # G7282) for 30min at room temperature. Protein complexes were eluted from the beads with 20 μL of 1% SDS and quantified via DC protein Assay Kit (Bio-Rad # 5000111). To remove SDS during proteomic analysis by the mass spectroscopy, 1 microgram of eluted protein complexes sample was resolved by gel electrophoresis just long enough for the sample to enter the gel, followed by cutting the gel pieces containing the entire sample. The buffers used during in-gel digestion were 0.1M ammonium bicarbonate prepared in sterile ddH2O (Buffer A) and 0.1M aqueous ammonium bicarbonate/acetonitrile (1:1 by volume, Buffer B). The gel pieces were destained by 30% methanol for 2 hours, partially dried in Buffer B for 30min, reduced with 10mM DTT in Buffer A for 30min, and dried again in Buffer B for an additional 3min with shaking at room temperature with end-over-end rotation. Then, the gel pieces were incubated with 50mM iodoacetamide in Buffer A to alkylate proteins with shaking in the dark for 30min. Next, gel pieces were crushed into small pieces and dried in Speed Vac for 20 minutes. The gel pieces were rehydrated in Buffer A and digested with Trypsin/LysC overnight at 37°C in a shaking incubator. After trypsin digestion, the solution was carefully removed into a clean tube, and the gel pieces were incubated with 0.1% TFA in 60% acetonitrile for 30min at 37°C in a shaking

incubator, carefully remove the solution and pool it with solution from last step. The process was repeated twice and the collected solution was dried in Speed Vac. Desalted peptides were labeled with TMT (6-plex) reagents following manufacture's protocol. Labeling of samples with TMT reagents was completed with the following design: 126 (negative control replicate 1 blocked by JF 594); 127 (negative control replicate 2 blocked by JF 594); 128 (negative control replicate 3 blocked by JF 594); 129 (sample replicate 3); 130 (sample replicate 1); 131 (sample replicate 2). Mass spectrometry and data analysis was performed as previously described(Won and Martin, 2018).

Western Blotting

Gels were transferred to methanol-activated Immobilon-FL membrane (Millipore) in the transfer buffer (25 mM Tris-base, 192 mM glycine, 10% methanol) at 100 V for 2 h. Proteins were probed with antibodies listed in the Key Resources Table for 16 h at 4 °C and then incubated with corresponding secondary antibodies for 1 hour at room temperature. Blots were developed by Clarity Max™ Western ECL Substrate (Bio- Rad), and then the Chemiluminescence was detected by an Azure c600 imager (Azure Biosystems) or ChemiDoc Touch imaging system (Bio-Rad); images were quantified using Bio-Rad Image Lab software.

Acknowledgements

We would like to thank Zhangyuan Yin for Chemidoc analysis. Financial support was provided by the National Institutes of Health DP2 GM114848, T32 GM008597 Chemical Biology Interfaces Training Grant (S.E.H.), S10 OD021619 (Orbitrap Fusion Lumos Tribrid Mass Spectrometer), and the University of Michigan.

Chapter 3 Conclusion and Future Directions

Conclusion

In this dissertation, we profiled native Scribble interactions across defined cellular contexts by CRISPR/Cas9 genome engineering to produce cells enconding a Scribble-HaloTag fusion. Inducible expression of the EMT-TF Snail eliminates cell polarity, mislocalizes Scribble-HaloTag, and promotes YAP nuclear localization. Halo-ligand affinity purification and mass spectrometry identified the Src family kinase (SFK) YES1 as a mislocalized Scribble-interaction partner. Like other SFK members, YES1 undergoes large configuration rearrangement to switch from a 'closed' inactive state to 'open' active state following activation by upstream signals (Boggon and Eck, 2004). Using conformation-specific SFK inhibitors, we discover that mislocalized Scribble interacts with YES1 in the active αC-helix in (open) conformation, while membrane localized but cell-cell junction excluded Scribble preferentially interacts with YES1 in the inactive αC-helix out (closed) conformation (**Figure 3.1**). Through using multiple chemical biology approaches, my dissertation finds that when Scribble is depleted from cells, YAP phosphorylation at Tyr 357 is reduced. In addition, Scribble-dependent scaffolding of conformationally active YES1 contributes to Snail-driven YAP-Y357 phosphorylation, a signal for nuclear localization.

In summary, taking advantage of multiplex chemical biology approaches, we identify a novel role of Scribble in the regulation of Wnt signaling pathways. We find that initiation of YES1 kinase activity is one of the mechanisms by which Scribble use to mediate YAP-Y357

phosphorylation. On the other hand, our discovery also illustrates one possible mechanism that many epithelial cancer cells may use to activate YES1, and suggests the crosstalk between tumor suppressor genes and proto-oncogenes.

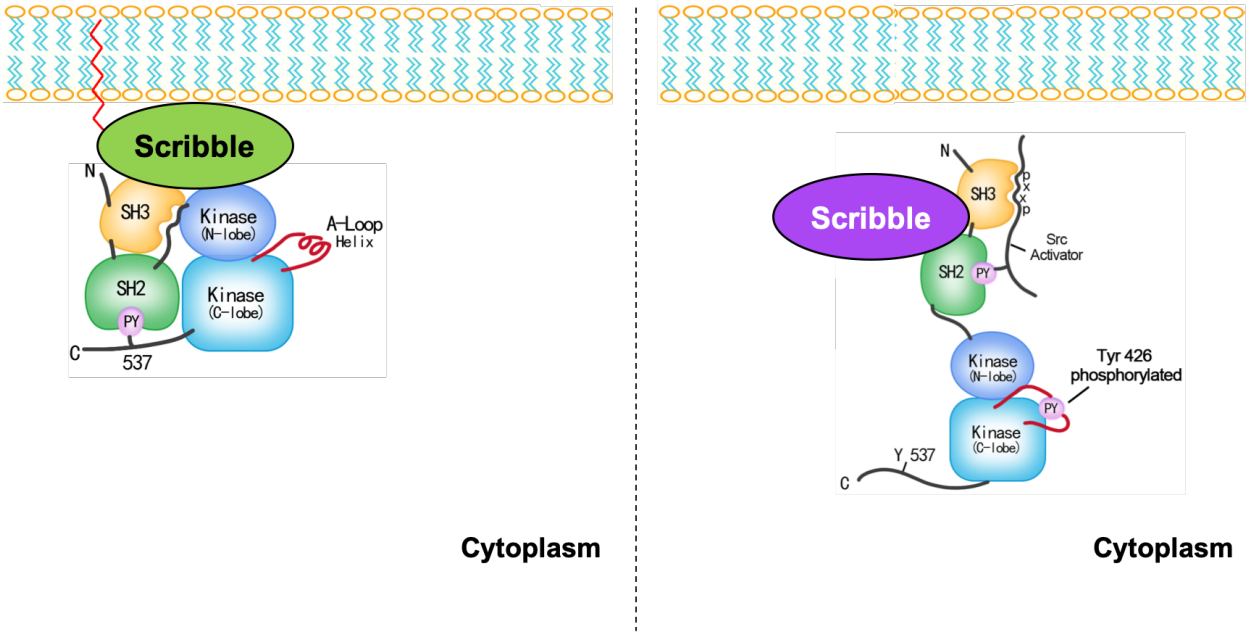

Figure 3.1 Summary of Scribble and YES1 interaction.

Membrane anchored, but cell-cell junction excluded Scribble preferentially associated with inactive YES1, while cytosolic Scribble can only interact with active YES1.

Future Directions

Map Interaction Domains Between Scribble and YES1

Although we discovered and validated Scribble and YES1 interaction, the domain that enables Scribble to interact with YES1 is still unknown. In addition, whether the membrane associated Scribble and its cytosolic counterpart use the same domain to interact with YES1 is unclear. It is clearly important to map the domain of membrane associated and cytosolic Scribble

that mediate Scribble and YES1 interaction, respectively. To this end, we generated truncated versions Scribble mutants to determine which domain of Scribble is required for YES1 interaction (**Figure 3.2**). Once the interaction domain is determined, that Scribble domain and YES1 could be expressed and purified in E.coli cells for in vitro pull-down assays to explore whether Scribble-YES1 is direct or indirect.

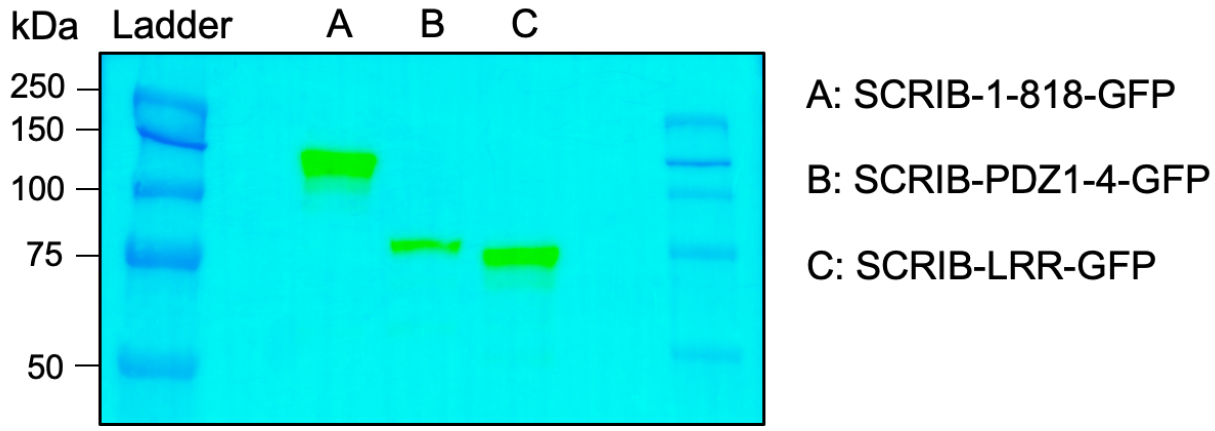

Figure 3.2 Expression and validation of truncated versions of Scribble to map the domain of YES1 interaction.

Potential Interaction of Scribble and Other Src Family Kinases

We predict that Scribble can also interact with other members of Src family kinases as all the members are highly homologous in structure (Boggon and Eck, 2004), unless the interaction with YES1 is mediated via the unique domain of YES1. We hypothesize that the Scribble and SFKs interaction will be related to the particular biological contexts such as specific cell cycles, developmental stages and cell types. To test our hypothesis, it is also relevant to co-express other SFKs with Scribble in 293T cells and perform the same Co-IP experiments described above to validate their interaction (**Figure 3.3**).

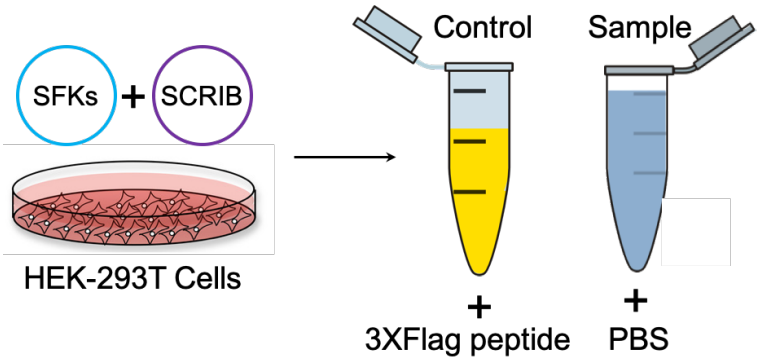

Figure 3.3 Schematic of Co-IP of Scribble with other SFKs in HEK-293T cells.

Integrate Biological Functions of Scribble and YES1 Interaction

In HEK-293T cells, we find that membrane associated Scribble interacts with inactive YES1 to facilitate its Tyr 426 phosphorylation and subsequent activation (**Figure 2.25**). However, whether similar effect exist with endogenous levels of YES1 in cells remains unknown. Since no specific anti-YES1 Try 426 phosphorylation antibody is commercially available, we propose to use CRISPR-Cas9 mediated genome editing to insert a C-terminal GFP fusion at the endogenous YES1 genomic locus in HEK-293T cells. Next, we could then co-express wild type Scribble, enrich YES1 through GFP pull down, and detect YES1 Tyr 426 phosphorylation level. However, HEK-293T cells are not a cancer cell line. Therefore, we will also access whether similar results are valid also in other cell lines, particularly in the cancer cell lines.

Furthermore, it has been reported that YES1 can be activated through upstream phosphatases (Sen and Johnson, 2011). Our affinity purification mass spectrometry also identified several protein tyrosine phosphatases as the potential Scribble interactors, including PTPN13 and PTP-PEST. Interestingly, PTPN13 has been reported to repress Src kinase activity

(Glondu-Lassis et al., 2010) while PTP-PEST to activate Src kinase activity (Chellaiah and Schaller, 2009). We speculate that Scribble and YES1 interaction might be bridged by these phosphatases. To validate our hypothesis, we will first validate their interaction with Scribble using the same methods described above. Once we confirm the interaction of Scribble with PTPN13 and PTP-PEST, we next will create a stable HEK-293T cell line that overexpress Scribble and YES1. Then we will introduce doxycycline inducible cassettes into this cell line to induce PTPN13 and PTP-PEST expression, respectively. Finally, the YES1 phosphorylation at Tyr 426 will be analyzed and compared.

We also find that cytosolic Scribble can only interact with active YES1 (**Figure 2.23**). However, the consequences of such interaction are not known. We hypothesize that Scribble may function as a scaffold facilitating YES1 substrate recognition and subsequent phosphorylation. To test our hypothesis, we firstly plan to confirm the formation of triple protein complex including cytosolic Scribble, active YES1 and YES1 substrate such as YAP or beta catenin. Our preliminary data demonstrates that both cytosolic Scribble and active YES1 can be detected in the beta-catenin pull down sample (**Figure 3.4**). For unknown reasons, we did not observe similar result in the YAP pull down sample, suggesting that further optimization of YAP co-immunoprecipitation is still needed.

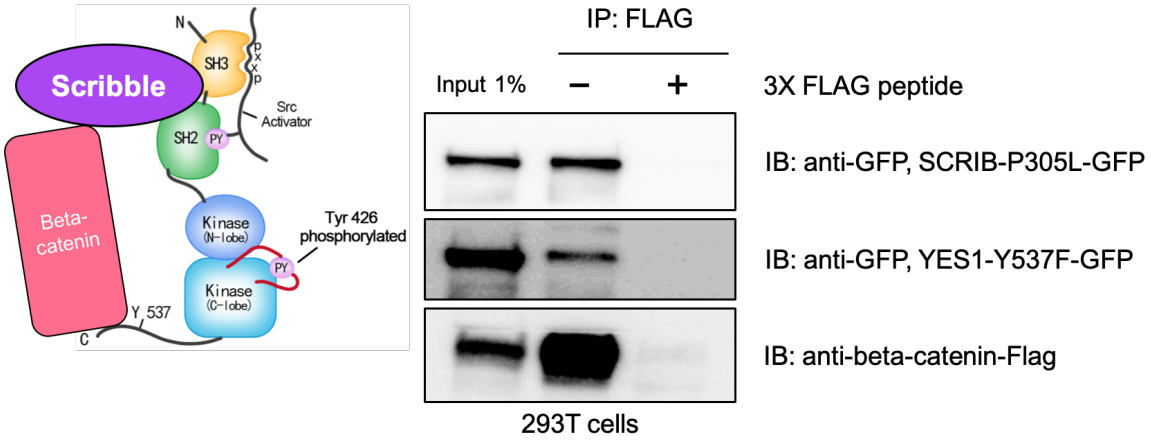

Figure 3.4 Cytosolic Scribble may form a triple complex with active YES1 and beta-catenin.

However, it is still uncertain whether the result observed in **Figure 3.4** is because cytosolic Scribble, active YES1, and beta catenin form a triple complex, or whether each one can independently interact with the other two. To further validate this, we could perform sequential co-immunoprecipitation to assay whether the triple complex contains cytosolic Scribble, active YES1 and beta-catenin exists or not. Next, we will perform mass spectrometry to compare the YAP and beta-catenin phosphorylation rates from the 293T cells expressing wild type and cytosolic Scribble.

Significance

Scribble has previously been shown to interact with a variety of proteins, linking it to a diverse set of biological processes. We identified and validated YES1, a member of Src family kinases, as a novel interactor of Scribble using multiple chemical biology approaches. To further understand the structural and biochemical basis of Scribble and YES1 interaction, we took advantage of the conformation-specific Src family kinase inhibitors to investigate the impact of

the quaternary structure changes on Scribble and YES1 interaction. We found and confirmed that YES1 kinase adopts different conformation to interact with Scribble, depending on the subcellular localization of Scribble. Based on these results, the Scribble-YES1 interaction represents a unique complex model to regulate the protein-protein interaction. Our study also demonstrates that abnormal subcellular localization of the tumor suppressor protein results in aberrant and disease-contributing interactions in human cancers.

Appendices

Appendix A: All Protein IDs from MS with Scribble as Bait

Table 1 List of Potential Interactors of Scribble.

Accession	Average Ratio	Ratio: Replicate 01	Ratio: Replicate 02	Ratio: Replicate 03
F1PPR3	15.23	4.58	39.58	1.54
F1Q3S9	11.68	1.99	29.68	3.38
F1PHS5	9.91	13.95	12.86	2.91
F1PPA1	9.29	18.49	4.88	4.49
E2RD95	8.84	12.58	6.87	7.07
F1P7L9	8.71	18.80	4.20	3.14
F1P9J3	8.65	19.91	3.94	2.09
J9JHR4	8.46	15.98	8.23	1.17
F1Q147	8.32	13.33	7.34	4.29
F1PVV7	8.09	16.03	5.80	2.44
E2RB62	8.07	16.36	6.08	1.77
F1PLS4	7.43	14.12	6.58	1.57
F1PFZ5	7.20	19.56	0.86	1.17
F1PRN2	7.15	12.56	4.92	3.98
J9P969	6.92	11.68	4.77	4.31
P33724	6.84	9.30	7.82	3.41

F6Y3P9	6.69	13.59	4.34	2.13
F1PGI1	6.54	16.77	0.77	2.09
P62872	6.48	9.03	4.81	5.59
E2QUR8	6.45	10.85	4.49	4.02
J9P7P6	6.45	6.47	11.01	1.88
F1PGX1	6.35	11.75	3.27	4.05
E2QW54	5.95	11.97	3.46	2.42
F1PNG1	5.73	7.77	7.86	1.55
F1PVU1	5.69	1.68	13.75	1.63
Z4YHI2	5.66	10.26	4.22	2.50
F1PSB7	5.57	5.88	4.24	6.59
F1Q0N9	5.48	2.49	1.03	12.91
E2RMC0	5.27	4.41	9.73	1.66
J9NX28	5.24	4.81	0.37	10.55
F1PX71	5.15	10.21	2.34	2.90
P38400	4.95	6.91	2.66	5.28
E2RNJ6	4.81	7.33	6.04	1.07
E2R948	4.61	3.10	6.97	3.78
E2RJQ8	4.51	4.24	8.07	1.23
E2RC56	4.44	1.86	9.45	2.00
F2Z4N7	4.42	7.82	2.47	2.98
E2QXK6	4.36	4.90	6.96	1.23
A0A0N9JE84	4.26	7.69	2.49	2.60

E2RB38	4.02	7.88	0.28	3.91
J9NXT9	3.98	5.37	3.56	3.00
F1P8D5	3.91	3.51	5.50	2.73
F1PC72	3.75	2.66	4.25	4.34
F1Q4E3	3.49	7.37	1.45	1.64
F6PME1	3.38	2.73	0.40	7.02
J9NUK3	3.34	7.72	1.39	0.90
E2QWL1	3.27	5.69	1.38	2.72
E2R0G4	3.26	3.96	3.67	2.15
Q6TEQ7	3.24	4.46	0.82	4.43
E2RER0	3.18	1.60	7.00	0.93
E2R2M7	3.18	2.88	2.31	4.35
E2RDF9	3.16	1.53	6.43	1.52
E2QWU0	3.15	3.49	0.93	5.03
E2RMY0	3.11	1.83	5.53	1.98
E2R428	3.08	4.54	1.15	3.56
A0A1W2NC67	3.08	1.31	6.18	1.74
F1PWH2	3.07	4.35	3.59	1.25
F1PVP9	3.00	1.77	5.71	1.51
E2RL95	2.99	2.67	4.93	1.36
E2R5G6	2.99	4.25	1.20	3.52
B6V8E6	2.95	1.25	5.66	1.95
F1Q1J6	2.93	1.76	4.97	2.07

E2RFE1	2.93	2.48	4.36	1.96
F1PPM7	2.93	2.68	5.06	1.05
E2RL19	2.90	1.65	5.24	1.79
J9P8A4	2.89	1.10	5.79	1.77
Q9N0Y3	2.86	6.68	1.68	0.23
E2RKA8	2.85	2.05	4.65	1.85
E2QY54	2.82	1.71	5.30	1.43
F1P9T0	2.81	1.96	4.54	1.94
F1PQS3	2.77	4.14	1.61	2.56
J9NSJ8	2.77	4.92	2.85	0.53
E2RKV3	2.76	2.22	2.74	3.33
E2RME9	2.69	1.69	4.56	1.82
F1PQ40	2.66	1.37	3.76	2.85
E2R0D5	2.62	4.62	1.78	1.46
E2RGI7	2.60	1.18	2.55	4.06
F1PZJ7	2.56	1.55	4.06	2.08
E2QXV5	2.54	2.28	3.49	1.84
F1P8K0	2.52	1.59	4.22	1.75
F1PWW0	2.50	2.32	3.34	1.85
E2RGN6	2.50	0.78	2.32	4.39
E2RPF2	2.47	1.12	4.91	1.38
E2RQ87	2.44	1.43	3.34	2.55
O97758	2.44	1.83	3.06	2.42

E2R1C4	2.44	1.17	2.47	3.66
E2RNQ5	2.43	1.95	3.74	1.61
E2R8R8	2.41	2.37	2.99	1.88
F6X8D7	2.41	2.73	1.86	2.64
E2R0S7	2.41	1.01	3.62	2.60
E2R1K2	2.40	2.47	3.01	1.71
E2RCF4	2.40	1.17	4.61	1.41
E2QUS0	2.39	1.46	4.38	1.33
F6UTN8	2.38	1.61	3.30	2.22
E2RBA4	2.37	1.18	4.53	1.41
J9P923	2.37	3.84	1.61	1.65
E2R434	2.37	2.30	3.09	1.70
Q5TJG6	2.35	1.38	3.64	2.03
E2R9C6	2.34	1.66	2.57	2.79
E2R0F2	2.34	3.49	1.45	2.08
J9P1H1	2.33	1.72	3.14	2.13
J9NUV0	2.32	1.69	3.30	1.97
F1PZ23	2.31	1.68	2.85	2.40
Q95KU4	2.29	1.24	2.00	3.64
E2R0A6	2.28	1.93	2.78	2.14
F1PLW6	2.28	3.40	2.87	0.56
E2RHC4	2.28	1.42	2.87	2.54
E2RPE5	2.27	1.84	2.47	2.50

F1P661	2.26	2.19	1.82	2.77
F1PHQ5	2.26	2.14	4.06	0.58
F1PBA1	2.26	2.52	1.99	2.26
J9P2Y3	2.25	3.15	1.04	2.55
F1Q424	2.24	1.91	2.12	2.70
A8W340	2.24	0.98	2.15	3.59
F6Y6T1	2.24	2.78	0.54	3.40
F1P9T5	2.24	2.29	3.14	1.27
G1K288	2.23	1.77	3.43	1.50
J9NZX5	2.23	1.75	3.46	1.49
E2RFI6	2.22	1.22	3.25	2.18
E2QUU5	2.19	1.78	2.87	1.93
F1PMK1	2.17	1.22	3.65	1.66
F1PUX1	2.16	1.87	3.53	1.08
J9NZX6	2.14	1.26	3.37	1.80
F1PFC2	2.14	1.95	2.99	1.48
F1PQ49	2.14	2.96	1.65	1.81
F1PVZ2	2.14	1.75	2.22	2.44
E2R3U9	2.12	1.50	3.69	1.17
F1PAN3	2.12	1.84	3.90	0.62
J9JHN1	2.10	1.49	2.85	1.96
F1PZ71	2.09	1.31	3.12	1.84
F1PXZ9	2.09	2.05	1.60	2.62

E2QUP1	2.09	1.31	2.00	2.96
F1PXD3	2.08	1.60	2.92	1.71
J9P530	2.08	2.15	2.98	1.11
F2Z4P2	2.07	1.38	2.35	2.46
E2RAB2	2.06	2.13	2.50	1.56
E2QYC7	2.04	2.31	2.36	1.46
E2RM09	2.04	1.71	3.15	1.28
E2R8A8	2.04	2.06	2.54	1.52
Q9N281	2.04	1.73	2.18	2.20
E2RGA2	2.03	1.22	2.96	1.92
F1PFK4	2.03	1.45	2.16	2.49
F1PGY9	2.03	2.04	1.75	2.29
J9NXE3	2.03	1.38	3.11	1.59
E2QYH2	2.02	1.49	3.43	1.15
E2RG47	2.02	1.86	2.85	1.35
E2QWF8	2.02	1.33	2.84	1.89
J9NZ05	2.02	2.54	2.60	0.92
F1PTR7	2.01	2.89	2.43	0.72
D0VWQ3	2.01	2.14	1.48	2.41
E2R580	2.01	1.47	3.14	1.41
J9P9G0	2.01	1.54	2.82	1.66
F1PSI7	2.00	2.18	1.94	1.89
E2QXF3	2.00	1.73	2.32	1.95

E2R3F9	2.00	1.94	2.08	1.97
J9NYH3	1.99	1.19	2.80	1.98
E2RTE7	1.99	1.22	2.50	2.24
J9NXV2	1.99	1.00	3.22	1.75
E2RBD1	1.99	1.24	1.54	3.18
F1P7B0	1.98	1.41	3.03	1.49
J9P2H0	1.98	1.96	1.80	2.17
E2RHY0	1.97	2.51	1.41	1.99
E2RJ79	1.97	1.96	2.35	1.60
O46674	1.97	1.66	2.60	1.65
F1PYI3	1.97	2.10	1.47	2.34
E2RR18	1.96	2.73	0.16	3.00
E2R0G3	1.96	1.53	1.77	2.57
F6X4J2	1.95	2.40	1.75	1.70
F1PKR9	1.95	1.17	2.86	1.82
J9P4R8	1.94	1.56	2.68	1.57
F1PKR6	1.94	1.81	2.62	1.38
E2REU7	1.93	1.65	2.71	1.44
J9NVC8	1.93	1.79	2.73	1.28
A0A077LQA5	1.93	2.93	2.40	0.47
F1PUE0	1.93	1.67	1.92	2.19
F1Q0H3	1.93	1.40	2.06	2.33
F1PIP0	1.92	2.55	0.59	2.64

E2QW28	1.92	1.43	2.36	1.98
E2QUR2	1.92	1.12	1.33	3.32
E2RJ35	1.92	1.97	2.07	1.72
F1PJ57	1.92	1.08	2.53	2.14
A0A1B1X469	1.91	1.54	1.89	2.30
E2RG67	1.91	2.17	1.72	1.83
F1PRL5	1.90	1.55	2.27	1.89
F1PU09	1.90	2.50	2.08	1.12
E2RQM6	1.88	2.31	2.36	0.98
E2RP67	1.88	2.03	2.13	1.47
F6XWM4	1.88	1.57	1.02	3.04
E2R4F5	1.87	1.71	2.21	1.69
J9P5N6	1.87	2.22	1.79	1.58
E2RT79	1.86	1.41	2.86	1.30
F1Q1T5	1.86	1.16	1.95	2.47
F6XRW3	1.85	1.79	2.48	1.29
E2RGF9	1.85	1.05	2.44	2.05
E2RJ03	1.83	1.08	2.87	1.55
F1PXU1	1.82	2.04	1.16	2.27
J9PAP8	1.82	1.08	1.98	2.41
F6V0W4	1.82	1.37	2.50	1.58
F1PS87	1.81	3.25	0.65	1.55
P18067	1.81	1.78	1.55	2.10

Q32KH6	1.81	2.08	2.14	1.22
E2QUB9	1.81	1.38	2.31	1.74
E2RMN6	1.81	0.87	2.66	1.90
F6V8G4	1.81	0.94	1.77	2.72
E2QYG6	1.81	1.73	1.30	2.39
E2RP05	1.81	1.50	1.77	2.14
F1PSK6	1.80	2.73	0.90	1.78
P51147	1.80	1.55	2.19	1.67
F2Z4Q1	1.79	1.44	2.38	1.56
E2RMR3	1.79	1.33	2.26	1.78
E2R2U3	1.79	1.16	2.52	1.69
F1PIS7	1.78	1.43	2.37	1.55
F1PQN3	1.78	1.87	1.65	1.82
F2Z4N3	1.78	1.43	1.83	2.08
E2RL90	1.78	1.11	2.29	1.93
E2QYF3	1.78	1.48	2.00	1.85
F1PGD7	1.78	1.47	1.68	2.18
F1PWP9	1.78	1.59	2.26	1.47
F2Z4P3	1.77	1.47	1.93	1.89
E2RIQ8	1.76	2.38	1.46	1.44
E2QS08	1.76	1.16	1.29	2.82
F1PGT8	1.76	1.81	1.74	1.73
J9P098	1.76	1.98	0.63	2.67

F1PMA6	1.76	1.67	1.28	2.32
J9P425	1.76	1.97	2.05	1.24
F1PFC6	1.75	1.71	1.53	2.02
E2RHE9	1.74	1.14	2.56	1.53
J9P5A8	1.74	2.08	1.14	2.01
F1PIY7	1.73	1.74	2.24	1.22
E2RSI6	1.73	2.53	1.32	1.33
E2RMK6	1.72	1.98	2.10	1.10
J9NSW5	1.72	1.15	1.95	2.06
E2RQV7	1.72	2.31	0.98	1.85
E2QWV0	1.71	1.55	2.06	1.53
F6UWL4	1.71	1.43	2.67	1.05
Q5TJE9	1.71	1.96	1.68	1.50
F1PP86	1.71	1.89	1.34	1.91
J9P0B2	1.71	0.95	0.84	3.33
F1PEA6	1.71	1.55	2.43	1.15
E2RPW8	1.71	1.09	2.04	1.99
J9JHI1	1.70	2.32	0.65	2.14
E2R0Y5	1.70	1.23	2.48	1.38
E2RH47	1.69	1.46	2.09	1.53
E2R4L0	1.69	1.36	0.85	2.86
D0VWQ5	1.69	1.64	1.57	1.84
E2RIA1	1.68	1.53	1.99	1.54

F1PCQ3	1.67	1.49	1.23	2.30
E2RH41	1.67	1.36	2.19	1.47
F1PHQ0	1.67	2.00	1.43	1.57
E2RLX2	1.67	1.11	2.13	1.77
A0A1W2NCW3	1.66	1.62	1.64	1.73
E2QYD8	1.66	1.65	0.98	2.37
J9NW12	1.66	1.21	2.49	1.28
F1PMR9	1.65	1.45	0.49	3.01
E2RQK4	1.65	1.27	1.64	2.04
P61007	1.65	1.67	1.20	2.08
P63273	1.65	1.78	1.62	1.55
F6Y732	1.65	1.13	1.94	1.87
E2RLE2	1.65	1.28	2.06	1.60
F1PGI3	1.64	1.88	1.69	1.36
J9NZF2	1.64	1.52	2.06	1.34
F1Q2A2	1.64	0.93	1.94	2.04
E2QWU2	1.64	1.17	0.89	2.86
E2RHZ3	1.64	1.01	2.34	1.56
E2RJT7	1.64	1.21	1.42	2.28
E2R9I0	1.63	0.97	2.21	1.72
F1Q1G9	1.63	1.73	1.93	1.23
E2QYZ9	1.63	1.29	2.12	1.48
E2RQ80	1.63	1.14	1.31	2.45

E2RHX1	1.63	1.76	1.65	1.48
E2RSR5	1.63	1.57	1.72	1.59
J9P0A6	1.63	1.45	2.05	1.38
H9GW76	1.63	1.10	1.79	1.99
F2Z4N5	1.62	1.67	1.47	1.73
E2RST6	1.62	1.51	2.31	1.03
F1PJ65	1.62	2.38	1.56	0.90
F6UTB0	1.61	1.06	1.41	2.37
E2R4I0	1.61	1.03	2.00	1.81
F1PK90	1.61	1.17	1.65	2.02
E2RIJ7	1.61	1.68	2.01	1.14
A0A1B1X461	1.61	1.22	2.18	1.43
E2REK3	1.61	1.93	1.18	1.71
E2RAU5	1.60	0.86	0.35	3.61
F6UX21	1.60	1.54	1.67	1.60
J9NXM6	1.60	1.45	1.66	1.69
F1Q1K6	1.60	1.33	1.74	1.72
F1P969	1.59	2.29	1.05	1.44
E2RPQ0	1.59	1.45	1.28	2.04
E2REZ9	1.58	1.54	2.07	1.14
F1PKS3	1.58	1.96	1.39	1.39
Q6YKA4	1.58	0.86	2.36	1.51
E2RL34	1.58	1.28	1.70	1.75

F6Y5H1	1.58	1.67	1.12	1.94
E2R3J4	1.58	1.47	1.08	2.18
A1XD97	1.58	0.97	1.95	1.80
E2R1J6	1.57	2.18	0.92	1.62
J9PBD3	1.56	1.40	1.35	1.94
E2R7T9	1.56	1.22	1.74	1.72
J9NTD9	1.56	1.14	1.29	2.25
E2RFF1	1.56	1.43	1.91	1.34
E2RHH4	1.56	1.24	1.68	1.76
E2RHL4	1.56	1.42	0.29	2.95
E2RIJ3	1.55	1.68	1.40	1.58
F6UMQ8	1.55	1.45	1.83	1.38
E2QWK8	1.55	1.08	2.33	1.25
E2RQH0	1.55	1.79	1.71	1.15
E2R9V0	1.55	1.24	1.06	2.34
E2QZG2	1.54	1.59	1.62	1.41
F1PC88	1.54	0.85	1.40	2.37
F1PTZ9	1.54	1.10	1.88	1.64
F1PV47	1.54	2.14	1.43	1.05
P33731	1.53	1.44	1.61	1.55
E2RJ06	1.53	1.12	1.72	1.76
F6Y8P9	1.53	2.07	0.47	2.05
F1PTP6	1.53	2.58	1.08	0.92

F1PU93	1.52	1.21	0.58	2.77
F1PGL4	1.52	1.20	1.01	2.33
E2RJN1	1.52	1.92	1.38	1.25
J9NTS2	1.52	1.44	1.38	1.73
J9NYU5	1.51	1.17	1.19	2.18
P62825	1.51	1.54	1.48	1.52
E2RBH4	1.51	1.33	1.29	1.91
E2QW25	1.51	1.08	1.30	2.14
Q9MYU8	1.51	1.76	1.23	1.53
E2RNB0	1.50	1.17	1.41	1.93
F2Z4N2	1.50	1.13	0.95	2.42
E2REW3	1.50	1.45	1.40	1.65
E2R8D6	1.50	1.57	1.53	1.40
F1PTP3	1.50	1.18	1.79	1.51
J9NZE0	1.49	1.39	1.48	1.61
E2R0Y4	1.49	1.49	1.35	1.63
J9P398	1.49	1.04	1.63	1.80
F1Q1X9	1.49	1.18	1.60	1.69
E2RDL8	1.48	1.06	1.06	2.34
E2RTC3	1.48	1.15	1.57	1.74
F1PHR6	1.48	1.69	1.39	1.37
E2RFA3	1.48	0.94	1.84	1.65
E2RIA8	1.48	1.37	0.91	2.15

E2RNL1	1.48	1.74	0.68	2.01
E2RP92	1.48	1.11	0.97	2.35
E2RBH1	1.47	2.16	0.81	1.46
J9P326	1.47	1.47	1.22	1.73
J9P0V9	1.47	1.49	1.74	1.18
J9P780	1.47	1.53	1.04	1.84
F1PDV9	1.47	1.12	1.52	1.77
E2RFR0	1.46	1.22	1.29	1.88
E2R266	1.46	2.57	0.83	0.99
J9P6V4	1.46	1.72	1.35	1.31
E2R149	1.46	1.70	1.38	1.29
J9NRX5	1.45	1.02	1.01	2.34
F1PNM2	1.45	1.67	1.04	1.65
E2RIV1	1.45	1.82	0.88	1.64
E2R4X9	1.45	0.86	0.92	2.56
F1PGL2	1.44	1.32	1.02	1.99
F1PTK1	1.44	1.32	1.15	1.85
E2RM68	1.44	0.73	2.02	1.57
E2QW27	1.43	1.96	0.27	2.06
F1PQ68	1.43	1.92	1.53	0.83
F1PNF3	1.42	1.66	0.77	1.84
E2RHU5	1.42	1.26	0.78	2.22
F1PYL5	1.42	1.05	1.50	1.72

J9P9C6	1.42	0.98	1.34	1.94
E2RRB7	1.42	1.68	1.53	1.05
E2RLL6	1.42	1.23	1.08	1.95
E2R6L9	1.42	1.27	1.78	1.20
F1PRE0	1.41	1.39	1.35	1.51
E2QYT6	1.41	1.31	1.28	1.64
E2RET3	1.41	1.21	1.48	1.55
E2RQE5	1.41	1.25	1.40	1.57
E2RN68	1.40	1.53	1.54	1.14
F1PUB9	1.40	0.76	1.11	2.33
F1PKI0	1.40	1.12	0.67	2.40
E2RQ08	1.39	1.33	1.23	1.62
F1PVW0	1.39	1.53	0.49	2.15
F1Q0S9	1.39	1.22	1.24	1.71
E2RMQ0	1.39	1.67	0.87	1.62
E2QW80	1.39	1.39	1.61	1.15
F1Q212	1.38	1.20	1.15	1.80
F1Q0B0	1.38	0.80	0.85	2.50
J9JHP5	1.38	1.73	0.80	1.60
E2RQL0	1.37	1.25	1.25	1.63
E2R8S0	1.37	1.30	1.63	1.19
F1PVY2	1.37	1.63	1.10	1.37
E2R1X1	1.37	1.04	1.37	1.69

E2R0L9	1.36	1.60	0.27	2.22
F6XH70	1.36	1.38	1.35	1.34
E2QW69	1.36	1.46	0.91	1.69
E2RKY3	1.35	0.92	1.27	1.87
E2RN03	1.35	1.13	1.06	1.86
F6XRT0	1.35	1.22	1.45	1.38
E2QSF4	1.35	1.40	1.37	1.28
F2Z4Q5	1.35	1.48	1.05	1.51
E2RRT4	1.34	0.97	1.57	1.49
E2RS43	1.34	1.28	1.01	1.74
F1PS20	1.34	1.40	1.24	1.39
E2RDB9	1.34	2.29	0.57	1.16
E2RQV6	1.33	1.12	1.18	1.71
F1PR36	1.33	1.66	0.66	1.68
F1Q3W0	1.33	1.12	1.02	1.86
F1PAG7	1.33	1.44	1.26	1.30
F1PAG0	1.33	1.12	1.55	1.31
E2RB90	1.33	1.04	1.61	1.32
J9P019	1.33	1.17	1.55	1.25
F1Q331	1.32	1.07	0.59	2.31
E2RIW7	1.32	1.45	0.71	1.80
E2RB79	1.32	1.33	0.68	1.96
E2RFV7	1.32	1.20	0.72	2.04

F1PAW8	1.32	1.14	1.01	1.81
E2RBC3	1.31	2.01	1.07	0.87
E2RAA0	1.31	1.13	1.13	1.69
F1PZ47	1.31	1.69	1.09	1.16
E2QSS3	1.31	1.32	1.19	1.41
E2QWV5	1.31	0.64	1.24	2.05
E2QUJ0	1.31	1.04	1.60	1.28
F1PLV2	1.31	1.52	1.03	1.36
E2R6K5	1.29	1.44	0.28	2.16
F1PUX4	1.29	1.06	0.75	2.07
J9P8D6	1.29	1.07	0.96	1.84
E2QU53	1.29	1.38	1.03	1.46
F1PRR3	1.29	1.03	1.56	1.28
Q5TJF3	1.29	0.98	1.24	1.66
F2Z4P4	1.29	1.39	0.94	1.53
E2RSD0	1.29	1.57	1.06	1.23
E2R8L3	1.29	1.08	1.21	1.57
F1PV59	1.28	1.01	1.34	1.49
F1PEI3	1.28	0.80	1.11	1.92
J9P2W1	1.28	1.34	0.77	1.71
F1PC28	1.27	1.07	1.43	1.33
J9NTC9	1.27	1.29	0.96	1.56
E2R541	1.27	1.16	1.04	1.61

E2RF17	1.27	1.17	1.31	1.33
E2RR58	1.26	1.17	0.45	2.17
F1PKF6	1.26	0.92	0.94	1.91
E2RBB4	1.26	1.06	1.64	1.06
Q00004	1.25	1.28	0.42	2.05
E2RQM9	1.25	1.54	1.12	1.09
E2RFJ7	1.25	1.73	0.97	1.06
E2QYH6	1.25	1.65	0.34	1.76
E2RR33	1.25	0.95	0.99	1.80
E2R7L0	1.24	1.07	1.00	1.66
E2RL65	1.24	0.87	1.10	1.76
D0VWQ4	1.24	1.22	1.07	1.44
E2RNQ2	1.24	1.41	1.33	0.98
E2RSU3	1.24	0.79	1.07	1.87
E2RLP4	1.23	1.13	0.95	1.63
E2RCX0	1.23	1.54	0.97	1.19
F1PAW6	1.23	1.61	0.62	1.47
E2R0M5	1.21	1.58	1.09	0.97
F1PBS6	1.21	1.52	0.77	1.35
E2R345	1.21	1.39	1.01	1.23
J9NVB9	1.20	1.32	1.00	1.29
E2RCM8	1.20	1.51	0.87	1.23
J9NSI3	1.20	1.14	1.06	1.39

E2RMM3	1.20	0.99	0.69	1.91
F1P818	1.19	0.97	0.98	1.63
J9JHA1	1.19	1.36	0.55	1.66
F1PGB6	1.19	0.89	0.61	2.06
E2RNA4	1.19	1.23	0.80	1.52
F1PL97	1.18	1.85	0.93	0.76
F1PLR0	1.18	1.17	0.64	1.73
E2R6S8	1.18	0.80	1.21	1.52
E2R0K4	1.18	1.41	0.36	1.77
E2R655	1.17	1.35	0.53	1.64
E2RSV0	1.17	1.32	0.50	1.70
F1PI93	1.17	1.33	1.23	0.95
E2RGM1	1.17	0.66	1.28	1.56
F1Q264	1.17	0.89	1.14	1.47
E2R3H7	1.16	1.87	0.56	1.05
F1PRL0	1.15	1.09	1.15	1.23
F1PWE6	1.15	1.78	0.55	1.11
E2RCI5	1.14	1.23	0.74	1.46
E2RL17	1.14	1.40	0.96	1.05
E2RC21	1.13	1.93	0.68	0.77
E2RQN7	1.13	1.16	0.57	1.65
F1P8H7	1.13	1.33	0.94	1.11
E2QYC2	1.13	1.52	0.62	1.24

E2RN80	1.12	0.99	1.05	1.32
E2R2M6	1.12	1.11	0.44	1.81
F1PDB4	1.11	0.84	0.88	1.59
E2RA48	1.10	0.89	1.13	1.28
F1PID8	1.09	1.16	0.89	1.21
E2RE10	1.09	1.13	0.82	1.32
J9NVQ3	1.08	1.01	0.66	1.56
L7N0I7	1.07	1.10	0.49	1.61
E2QUQ3	1.06	1.21	0.42	1.55
E2R496	1.06	0.86	1.14	1.17
F1PFK6	1.05	1.43	0.92	0.79
E2RNV6	1.04	1.03	0.80	1.30
E2RQC9	1.04	0.90	0.49	1.71
E2QWH0	1.03	1.38	0.46	1.26
E2RRZ0	1.03	0.90	0.55	1.63
E2RGI3	1.01	0.95	0.74	1.33
E2RSP4	1.00	1.16	0.38	1.45
F1PHR2	1.00	1.22	0.63	1.15
J9P3X4	0.97	0.96	0.32	1.65
F1PBB3	0.97	1.99	0.35	0.57
F1Q2X3	0.96	0.72	0.71	1.44
F1P6B7	0.95	0.64	0.21	1.99
J9NZF6	0.94	0.69	0.39	1.73

E2R9J8	0.92	0.73	0.92	1.11
F6X637	0.90	0.98	0.28	1.45
E2REX8	0.86	0.97	0.24	1.38
E2R4B0	0.79	1.04	0.30	1.04
J9JHN5	0.74	0.54	0.61	1.06

Appendix B: Reagents Used in This Study

Table 2 List of Primers Used for Cloning and Mutagenesis.

Primers Name	Sequence 5'-3'
Guide sg01 canis Fwd	CACCGTGGGCCCCGTGCCCTCCTAG
Guide sg01 canis Rev	AAACCTAGGAGGGCACGGGGCCCA
Guide sg02 canis top	CACCGGGGAGGTTCTGGAGCCTCT
Guide sg02 canis bottom	AAACAGAGGCTCCAGAACCTCCCC
MDCK (L + R) HA Fwd	TACAGCCCAGACCTCTGCCAATGCCTACT
MDCK (L + R) HA Rev	TGTTCGACCTGCACGAGCTGGACCTGTT
Infusion primer MDCK Left HA_3X Flag Fwd	ACCATGATTACGCCAAGCTTTACAGCCCAGACC TCTGCCAAT
Infusion primer MDCK Left HA 3X Flag Rev	CCGTCATGGTCTTTGTAGTCGGAGGGCACGGG GCCCAG
Infusion primer 3X Flag loxP SV40 promoter EGFP loxP Fwd	GCCTGGGCCCCGTGCCCTCCGACTACAAAGAC CATGACGGTGAT
Infusion primer 3X Flag loxP SV40 promoter_EGFP_loxP Rev	AAGCCAGTACCGATTTCTGCGGTACCGGATAAC TTCGTATAGCAT

Infusion primer loxP HaloTag MDCK Right HA Fwd	ATACGAAGTTATCCGGTACCGCAGAAATCGGTACTGGCTTTCCAT
Infusion primer loxP HaloTag MDCK Right HA Rev	GGGAGGTTCTGGAGCCTCTAGCTCTGAAAGTACAGATCCTCAGT
Infusion primer HaloTag MDCK Right HA Fwd	AGGATCTGTACTTTCAGAGCTAGAGGCTCCAGAACCTCCCCT
Infusion primer HaloTag MDCK Right HA Rev	AGCTCGGTACCCGGGGATCCTGTTCGACCTGCACGAGCTG
Infusion primer Flag Snail T2A EGFP Fwd	TCGCCTGGAGAATTGGCTAGCGCCACCATGGATTACAAGGATGACGACGATAAGAGCCCGGGCGGCTCCCCGCGCTCTTTCCTCGTCAG
Infusion primer Flag Snail T2A EGFP Rev	TGCTCACCATTGGACCAGGGTTTTCTTCAACATCACCACAAGTGAGGAGAGAACCTCTACCTTCGCGGGGACATCCTGAGCAGC
Infusion primer T2A EGFP Fwd	CCCTGGTCCAATGGTGAGCAAGGGCGAGG
Infusion primer T2A EGFP Rev	CGCAACCCCAACCCCGGATCCTTACTTGTACAGCTCGTCCATGCC
YES1-GFP site mutagenesis-Q538E, P539E, G540I_Fwd	CTTCACTGCTACAGAGCCACAGTACGAGGAGATAGAAAATTTATGGGCCCGGGATCCA
YES1-GFP site mutagenesis-Q538E, P539E, G540I_Rev	TGGATCCCGGGCCCATAAATTTTCTATCTCCTCGTACTGTGGCTCTGTAGCAGTGAAG

YES1-GFP site mutagenesis-Y537F Fwd	TCCTGGCTGGAACTGTGGCTCTGTAGCAGT
YES1-GFP site mutagenesis-Y537F Rev	ACTGCTACAGAGCCACAGTTCCAGCCAGGA
YES1-Y537F site mutagenesis Fwd	TATAAATTTTCTCCTGGCTGATACTGTGGCTCTGTAGCAGTG
YES1-Y537F site mutagenesis Rev	CACTGCTACAGAGCCACAGTATCAGCCAGGAGAAAATTTATA

Table 3 List of Constructs Used in the Thesis.

Constructs Name	Source and Identifier
psPAX2	Addgene Plasmid Cat #12260
pMD2.G	Addgene Plasmid Cat #12259
pcDNA Flag Yap	Addgene Plasmid Cat #18881
pcDNA Flag beta Catenin	Addgene Plasmid Cat #16828
pUC57-FLAG-LoxP-GFP-LoxP-SNAP-TERT	Addgene Plasmid Cat #71391
pBS598 EF1alpha-EGFPcre	Addgene Plasmid Cat #11923
pCW57.1-Cas9	Addgene Plasmid Cat #50661
pPGS-hSNAIL.fl.flag	Addgene Plasmid Cat #25695
pLX304-YES1-Y537F	Addgene Plasmid Cat #51299
pEGFP-N1-YES1	Addgene Plasmid Cat #110497

pX330-U6-Chimeric_BB-CBh-hSpCas9	Addgene Plasmid Cat #42230
pUC19	Addgene Plasmid Cat #50005
pH6HTN His6HaloTag® T7 Vector	Promega Cat #G7971
pCW57.1-FLAG-Snail-T2A-EGFP	This paper N/A
pLX304-YES1-WT	This paper N/A
pEGFP-N1-YES1-Y537F	This paper N/A
pEGFP-N1-YES1-Q538E, P539E, G540I	This paper N/A
pcDNA 3.0-SCRIB-WT-Flag	This paper N/A
pcDNA 3.0-SCRIB-P305L-Flag	This paper N/A
pcDNA 3.0-SCRIB-WT-GFP	This paper N/A
pcDNA 3.0-SCRIB-P305L-GFP	This paper N/A

Table 4 List of Antibodies Used in the Thesis.

Antibodies	Source and Identifier
Goat polyclonal anti-SCRIB	Santa Cruz Biotechnology Cat# sc-11049
Rabbit monoclonal anti-beta-Actin	Cell Signaling Technology Cat# 4970

Rabbit monoclonal anti-YAP	Cell Signaling Technology Cat# 14074
Rabbit monoclonal anti-phospho-YAP-S127	Cell Signaling Technology Cat# 13008
Rabbit polyclonal anti-beta-Catenin	Cell Signaling Technology Cat# 9587
Rabbit monoclonal anti-non phospho-beta-Catenin (active)	Cell Signaling Technology Cat# 19807
Rabbit polyclonal phospho-Src Family (Tyr416)	Cell Signaling Technology Cat# 2101
Rabbit monoclonal anti-GAPHD	Cell Signaling Technology Cat# 5174
Rabbit monoclonal anti-GFP	Cell Signaling Technology Cat# 2956
Rabbit (DA1E) monoclonal IgG XP Isotype Control	Cell Signaling Technology Cat# 3900
Rabbit polyclonal anti-YAP (Y357)	Abcam Cat# ab62751
Mouse monoclonal anti-YES1	BD Transduction Laboratories™ Cat# 610376
Goat anti-Mouse IgG (H+L) Cross-Adsorbed Secondary Antibody, Alexa Fluor 594	Invitrogen Cat# A-11005 Cat# A-11005
Donkey anti-Goat IgG (H+L) Highly Cross-Adsorbed Secondary Antibody, Alexa Fluor Plus 594	Invitrogen Cat# A-32758 Cat# A-32758

Goat anti-Mouse IgG (H+L) Cross-Adsorbed Secondary Antibody, Alexa Fluor 488	Invitrogen Cat# A-11001 Cat# A-11001
Goat anti-Rabbit IgG (H+L) Cross-Adsorbed Secondary Antibody, Alexa Fluor 594	Invitrogen Cat# A-11012 Cat# A-11012
Goat anti-Mouse IgG (H+L) Cross-Adsorbed Secondary Antibody, HRP	Invitrogen Cat# G-21040 Cat# G-21040
Goat anti-Rabbit IgG (H+L) Cross-Adsorbed Secondary Antibody, HRP	Invitrogen Cat# G-21234 Cat# G-21234
Rabbit anti-Goat IgG (H+L) Secondary Antibody, HRP	Invitrogen Cat# 31402 Cat# 31402

Table 5 List of Critical Commercial Assays.

Antibodies	Source and Identifier
DC protein Assay	Bio-Rad Cat# 5000111
4x Laemmli Sample Buffer	Bio-Rad Cat# 1610747
Clarity Max™ Western ECL Substrate	Bio-Rad Cat# 1705062
Anti-FLAG® M2 Magnetic Beads	Sigma Aldrich Cat# M8823
Magne® HaloTag® Beads	Promega Cat# G7282

SureBeads(tm) Protein G Magnetic Beads	Bio-Rad Cat# 1614023
GFP-Trap Resin	ChromoTek Cat# gtma-10
TMTsixplex™ Isobaric Label Reagent Set	Thermo Scientific™ Cat# 90061
Lipofectamine™ LTX Reagent with PLUS™ Reagent	Thermo Scientific™ Cat# 15338100
Lipofectamine™ 3000 Transfection Reagent	Thermo Scientific™ Cat# L3000015
Trypsin	Promega Cat# V5113
FuGENE HD	Promega Cat# E2311
In-Fusion HD Cloning Plus kit	Takara Bio USA, Inc. Cat# 638909
Polybrene Infection / Transfection Reagent	Santa Cruz Biotechnology Cat# TR-1003-G
Control siRNA-A	Santa Cruz Biotechnology Cat# sc-37007
Scrib siRNA (h)	Santa Cruz Biotechnology Cat# sc-36466
c-Yes siRNA (h)	Santa Cruz Biotechnology Cat# sc-29860
PepMute™ siRNA Transfection Reagent	SignaGen Laboratories Cat# SL100566
QuickChange II XL Site-Directed Mutagenesis Kit	Agilent Technologies Cat#: 200522

Bibliography

Albertson, R., Chabu, C., Sheehan, A., and Doe, C.Q. (2004). Scribble protein domain mapping reveals a multistep localization mechanism and domains necessary for establishing cortical polarity. J Cell Sci *117*, 6061-6070.

Albertson, R., and Doe, C.Q. (2003). Dlg, Scrib and Lgl regulate neuroblast cell size and mitotic spindle asymmetry. Nat Cell Biol *5*, 166-170.

Arpin-Andre, C., and Mesnard, J.M. (2007). The PDZ domain-binding motif of the human T cell leukemia virus type 1 tax protein induces mislocalization of the tumor suppressor hScrib in T cells. J Biol Chem *282*, 33132-33141.

Audebert, S., Navarro, C., Nourry, C., Chasserot-Golaz, S., Lecine, P., Bellaiche, Y., Dupont, J.L., Premont, R.T., Sempere, C., Strub, J.M.*, et al.* (2004). Mammalian Scribble forms a tight complex with the betaPIX exchange factor. Curr Biol *14*, 987-995.

Barraclough, J., Hodgkinson, C., Hogg, A., Dive, C., and Welman, A. (2007). Increases in c-Yes expression level and activity promote motility but not proliferation of human colorectal carcinoma cells. Neoplasia *9*, 745-754.

Bilal, E., Alexe, G., Yao, M., Cong, L., Kulkarni, A., Ginjala, V., Toppmeyer, D., Ganesan, S., and Bhanot, G. (2010). Identification of the YES1 Kinase as a Therapeutic Target in Basal-Like Breast Cancers. Genes Cancer *1*, 1063-1073.

Bilder, D., and Perrimon, N. (2000). Localization of apical epithelial determinants by the basolateral PDZ protein Scribble. Nature *403*, 676-680.

Boeda, B., and Etienne-Manneville, S. (2015). Spectrin binding motifs regulate Scribble cortical dynamics and polarity function. Elife *4*.

Bonello, T.T., and Peifer, M. (2019). Scribble: A master scaffold in polarity, adhesion, synaptogenesis, and proliferation. J Cell Biol *218*, 742-756.

Brown, M.T., and Cooper, J.A. (1996). Regulation, substrates and functions of src. Biochim Biophys Acta *1287*, 121-149.

Chatterji, T., Varkaris, A.S., Parikh, N.U., Song, J.H., Cheng, C.J., Schweppe, R.E., Alexander, S., Davis, J.W., Troncoso, P., Friedl, P.*, et al.* (2015). Yes-mediated phosphorylation of focal adhesion kinase at tyrosine 861 increases metastatic potential of prostate cancer cells. Oncotarget *6*, 10175-10194.

Chen, B., Zheng, B., DeRan, M., Jarugumilli, G.K., Fu, J., Brooks, Y.S., and Wu, X. (2016). ZDHHC7-mediated S-palmitoylation of Scribble regulates cell polarity. Nat Chem Biol *12*, 686-693.

Chen, L., Cao, H., and Feng, Y. (2018). MiR-199a suppresses prostate cancer paclitaxel resistance by targeting YES1. World J Urol *36*, 357-365.

Cordenonsi, M., Zanconato, F., Azzolin, L., Forcato, M., Rosato, A., Frasson, C., Inui, M., Montagner, M., Parenti, A.R., Poletti, A.*, et al.* (2011). The Hippo transducer TAZ confers cancer stem cell-related traits on breast cancer cells. Cell *147*, 759-772.

Dow, L.E., Brumby, A.M., Muratore, R., Coombe, M.L., Sedelies, K.A., Trapani, J.A., Russell, S.M., Richardson, H.E., and Humbert, P.O. (2003). hScrib is a functional homologue of the Drosophila tumour suppressor Scribble. Oncogene *22*, 9225-9230.

Dow, L.E., Elsum, I.A., King, C.L., Kinross, K.M., Richardson, H.E., and Humbert, P.O. (2008). Loss of human Scribble cooperates with H-Ras to promote cell invasion through deregulation of MAPK signalling. Oncogene *27*, 5988-6001.

Dow, L.E., Kauffman, J.S., Caddy, J., Zarbalis, K., Peterson, A.S., Jane, S.M., Russell, S.M., and Humbert, P.O. (2007). The tumour-suppressor Scribble dictates cell polarity during directed epithelial migration: regulation of Rho GTPase recruitment to the leading edge. Oncogene *26*, 2272-2282.

Enkhbayar, P., Kamiya, M., Osaki, M., Matsumoto, T., and Matsushima, N. (2004). Structural principles of leucine-rich repeat (LRR) proteins. Proteins *54*, 394-403.

Fan, P.D., Narzisi, G., Jayaprakash, A.D., Venturini, E., Robine, N., Smibert, P., Germer, S., Yu, H.A., Jordan, E.J., Paik, P.K.*, et al.* (2018). YES1 amplification is a mechanism of acquired resistance to EGFR inhibitors identified by transposon mutagenesis and clinical genomics. Proc Natl Acad Sci U S A *115*, E6030-E6038.

Fang, Z., Yin, S., Sun, R., Zhang, S., Fu, M., Wu, Y., Zhang, T., Khaliq, J., and Li, Y. (2017). miR-140-5p suppresses the proliferation, migration and invasion of gastric cancer by regulating YES1. Mol Cancer *16*, 139.

Feigin, M.E., Akshinthala, S.D., Araki, K., Rosenberg, A.Z., Muthuswamy, L.B., Martin, B., Lehmann, B.D., Berman, H.K., Pietenpol, J.A., Cardiff, R.D.*, et al.* (2014). Mislocalization of the cell polarity protein scribble promotes mammary tumorigenesis and is associated with basal breast cancer. Cancer Res *74*, 3180-3194.

Friedl, P., and Wolf, K. (2003). Tumour-cell invasion and migration: diversity and escape mechanisms. Nat Rev Cancer *3*, 362-374.

Gardiol, D., Zacchi, A., Petrera, F., Stanta, G., and Banks, L. (2006). Human discs large and scrib are localized at the same regions in colon mucosa and changes in their expression patterns

are correlated with loss of tissue architecture during malignant progression. Int J Cancer *119*, 1285-1290.

Garmendia, I., Pajares, M.J., Hermida-Prado, F., Ajona, D., Bertolo, C., Sainz, C., Lavin, A., Remirez, A.B., Valencia, K., Moreno, H.*, et al.* (2019). YES1 Drives Lung Cancer Growth and Progression and Predicts Sensitivity to Dasatinib. Am J Respir Crit Care Med *200*, 888-899.

Grifoni, D., Garoia, F., Bellosta, P., Parisi, F., De Biase, D., Collina, G., Strand, D., Cavicchi, S., and Pession, A. (2007). aPKCzeta cortical loading is associated with Lgl cytoplasmic release and tumor growth in Drosophila and human epithelia. Oncogene *26*, 5960-5965.

Grzeschik, N.A., Parsons, L.M., Allott, M.L., Harvey, K.F., and Richardson, H.E. (2010). Lgl, aPKC, and Crumbs regulate the Salvador/Warts/Hippo pathway through two distinct mechanisms. Curr Biol *20*, 573-581.

Halder, G., and Johnson, R.L. (2011). Hippo signaling: growth control and beyond. Development *138*, 9-22.

Hamamura, K., Tsuji, M., Hotta, H., Ohkawa, Y., Takahashi, M., Shibuya, H., Nakashima, H., Yamauchi, Y., Hashimoto, N., Hattori, H.*, et al.* (2011). Functional activation of Src family kinase yes protein is essential for the enhanced malignant properties of human melanoma cells expressing ganglioside GD3. J Biol Chem *286*, 18526-18537.

Ivarsson, Y., Arnold, R., McLaughlin, M., Nim, S., Joshi, R., Ray, D., Liu, B., Teyra, J., Pawson, T., Moffat, J.*, et al.* (2014). Large-scale interaction profiling of PDZ domains through proteomic peptide-phage display using human and viral phage peptidomes. Proc Natl Acad Sci U S A *111*, 2542-2547.

Jin, Y., Huang, M., Wang, Y., Yi, C., Deng, Y., Chen, Y., Jiang, L., Wang, J., Shen, Q., Liu, R.*, et al.* (2016). c-Yes enhances tumor migration and invasion via PI3K/AKT pathway in epithelial ovarian cancer. Exp Mol Pathol *101*, 50-57.

Kleber, S., Sancho-Martinez, I., Wiestler, B., Beisel, A., Gieffers, C., Hill, O., Thiemann, M., Mueller, W., Sykora, J., Kuhn, A.*, et al.* (2008). Yes and PI3K bind CD95 to signal invasion of glioblastoma. Cancer Cell *13*, 235-248.

Knoblich, J.A. (2010). Asymmetric cell division: recent developments and their implications for tumour biology. Nat Rev Mol Cell Biol *11*, 849-860.

Lee, H.J., and Zheng, J.J. (2010). PDZ domains and their binding partners: structure, specificity, and modification. Cell Commun Signal *8*, 8.

Liu, H., Golebiewski, L., Dow, E.C., Krug, R.M., Javier, R.T., and Rice, A.P. (2010). The ESEV PDZ-binding motif of the avian influenza A virus NS1 protein protects infected cells from apoptosis by directly targeting Scribble. J Virol *84*, 11164-11174.

Marchetti, D., Parikh, N., Sudol, M., and Gallick, G.E. (1998). Stimulation of the protein tyrosine kinase c-Yes but not c-Src by neurotrophins in human brain-metastatic melanoma cells. Oncogene *16*, 3253-3260.

Michael, M., and Doherty, M.M. (2005). Tumoral drug metabolism: overview and its implications for cancer therapy. J Clin Oncol *23*, 205-229.

Michaelis, U.R., Chavakis, E., Kruse, C., Jungblut, B., Kaluza, D., Wandzioch, K., Manavski, Y., Heide, H., Santoni, M.J., Potente, M.*, et al.* (2013). The polarity protein Scrib is essential for directed endothelial cell migration. Circ Res *112*, 924-934.

Mohammad, R.M., Muqbil, I., Lowe, L., Yedjou, C., Hsu, H.Y., Lin, L.T., Siegelin, M.D., Fimognari, C., Kumar, N.B., Dou, Q.P.*, et al.* (2015). Broad targeting of resistance to apoptosis in cancer. Semin Cancer Biol *35 Suppl*, S78-S103.

Mohr, J., Dash, B.P., Schnoeder, T.M., Wolleschak, D., Herzog, C., Tubio Santamaria, N., Weinert, S., Godavarthy, S., Zanetti, C., Naumann, M.*, et al.* (2018). The cell fate determinant Scribble is required for maintenance of hematopoietic stem cell function. Leukemia *32*, 1211-1221.

Moreau, M.M., Piguel, N., Papouin, T., Koehl, M., Durand, C.M., Rubio, M.E., Loll, F., Richard, E.M., Mazzocco, C., Racca, C.*, et al.* (2010). The planar polarity protein Scribble1 is essential for neuronal plasticity and brain function. J Neurosci *30*, 9738-9752.

Nagasaka, K., Massimi, P., Pim, D., Subbaiah, V.K., Kranjec, C., Nakagawa, S., Yano, T., Taketani, Y., and Banks, L. (2010a). The mechanism and implications of hScrib regulation of ERK. Small GTPases *1*, 108-112.

Nagasaka, K., Pim, D., Massimi, P., Thomas, M., Tomaic, V., Subbaiah, V.K., Kranjec, C., Nakagawa, S., Yano, T., Taketani, Y.*, et al.* (2010b). The cell polarity regulator hScrib controls ERK activation through a KIM site-dependent interaction. Oncogene *29*, 5311-5321.

Nagasaka, K., Seiki, T., Yamashita, A., Massimi, P., Subbaiah, V.K., Thomas, M., Kranjec, C., Kawana, K., Nakagawa, S., Yano, T.*, et al.* (2013). A novel interaction between hScrib and PP1gamma downregulates ERK signaling and suppresses oncogene-induced cell transformation. PLoS One *8*, e53752.

Nakagawa, S., and Huibregtse, J.M. (2000). Human scribble (Vartul) is targeted for ubiquitin-mediated degradation by the high-risk papillomavirus E6 proteins and the E6AP ubiquitin-protein ligase. Mol Cell Biol *20*, 8244-8253.

Nakagawa, S., Yano, T., Nakagawa, K., Takizawa, S., Suzuki, Y., Yasugi, T., Huibregtse, J.M., and Taketani, Y. (2004). Analysis of the expression and localisation of a LAP protein, human scribble, in the normal and neoplastic epithelium of uterine cervix. Br J Cancer *90*, 194-199.

Navarro, C., Nola, S., Audebert, S., Santoni, M.J., Arsanto, J.P., Ginestier, C., Marchetto, S., Jacquemier, J., Isnardon, D., Le Bivic, A.*, et al.* (2005). Junctional recruitment of mammalian Scribble relies on E-cadherin engagement. Oncogene *24*, 4330-4339.

Osmani, N., Vitale, N., Borg, J.P., and Etienne-Manneville, S. (2006). Scrib controls Cdc42 localization and activity to promote cell polarization during astrocyte migration. Curr Biol *16*, 2395-2405.

Pearson, H.B., Perez-Mancera, P.A., Dow, L.E., Ryan, A., Tennstedt, P., Bogani, D., Elsum, I., Greenfield, A., Tuveson, D.A., Simon, R.*, et al.* (2011). SCRIB expression is deregulated in human prostate cancer, and its deficiency in mice promotes prostate neoplasia. J Clin Invest *121*, 4257-4267.

Pham, K., Shimoni, R., Charnley, M., Ludford-Menting, M.J., Hawkins, E.D., Ramsbottom, K., Oliaro, J., Izon, D., Ting, S.B., Reynolds, J.*, et al.* (2015). Asymmetric cell division during T cell development controls downstream fate. J Cell Biol *210*, 933-950.

Ran, F.A., Hsu, P.D., Wright, J., Agarwala, V., Scott, D.A., and Zhang, F. (2013). Genome engineering using the CRISPR-Cas9 system. Nat Protoc *8*, 2281-2308.

Rocha, C.R.R., Silva, M.M., Quinet, A., Cabral-Neto, J.B., and Menck, C.F.M. (2018). DNA repair pathways and cisplatin resistance: an intimate relationship. Clinics (Sao Paulo) *73*, e478s.

Rosenbluh, J., Nijhawan, D., Cox, A.G., Li, X., Neal, J.T., Schafer, E.J., Zack, T.I., Wang, X., Tsherniak, A., Schinzel, A.C.*, et al.* (2012). beta-Catenin-driven cancers require a YAP1 transcriptional complex for survival and tumorigenesis. Cell *151*, 1457-1473.

Sancier, F., Dumont, A., Sirvent, A., Paquay de Plater, L., Edmonds, T., David, G., Jan, M., de Montrion, C., Coge, F., Leonce, S.*, et al.* (2011). Specific oncogenic activity of the Src-family tyrosine kinase c-Yes in colon carcinoma cells. PLoS One *6*, e17237.

Sandilands, E., Brunton, V.G., and Frame, M.C. (2007). The membrane targeting and spatial activation of Src, Yes and Fyn is influenced by palmitoylation and distinct RhoB/RhoD endosome requirements. J Cell Sci *120*, 2555-2564.

Sato, A., Sekine, M., Virgona, N., Ota, M., and Yano, T. (2012). Yes is a central mediator of cell growth in malignant mesothelioma cells. Oncol Rep *28*, 1889-1893.

Schindler, T., Sicheri, F., Pico, A., Gazit, A., Levitzki, A., and Kuriyan, J. (1999). Crystal structure of Hck in complex with a Src family-selective tyrosine kinase inhibitor. Mol Cell *3*, 639-648.

Shen, Y., Chen, F., and Liang, Y. (2019). MicroRNA-133a inhibits the proliferation of non-small cell lung cancer by targeting YES1. Oncol Lett *18*, 6759-6765.

Sun, T., Yang, L., Kaur, H., Pestel, J., Looso, M., Nolte, H., Krasel, C., Heil, D., Krishnan, R.K., Santoni, M.J.*, et al.* (2017). A reverse signaling pathway downstream of Sema4A controls cell migration via Scrib. J Cell Biol *216*, 199-215.

Sun, Y., Aiga, M., Yoshida, E., Humbert, P.O., and Bamji, S.X. (2009). Scribble interacts with beta-catenin to localize synaptic vesicles to synapses. Mol Biol Cell *20*, 3390-3400.
Sun, Y., and Bamji, S.X. (2011). beta-Pix modulates actin-mediated recruitment of synaptic vesicles to synapses. J Neurosci *31*, 17123-17133.

Sundell, G.N., Arnold, R., Ali, M., Naksukpaiboon, P., Orts, J., Guntert, P., Chi, C.N., and Ivarsson, Y. (2018). Proteome-wide analysis of phospho-regulated PDZ domain interactions. Mol Syst Biol *14*, e8129.

Takeda, T., Yamamoto, H., Kanzaki, H., Suzawa, K., Yoshioka, T., Tomida, S., Cui, X., Murali, R., Namba, K., Sato, H.*, et al.* (2017). Yes1 signaling mediates the resistance to Trastuzumab/Lap atinib in breast cancer. PLoS One *12*, e0171356.

Tan, W., Lim, S.G., and Tan, T.M. (2015). Up-regulation of microRNA-210 inhibits proliferation of hepatocellular carcinoma cells by targeting YES1. World J Gastroenterol *21*, 13030-13041.

Tatosyan, A.G., and Mizenina, O.A. (2000). Kinases of the Src family: structure and functions. Biochemistry (Mosc) *65*, 49-58.

Tauzin, S., Chaigne-Delalande, B., Selva, E., Khadra, N., Daburon, S., Contin-Bordes, C., Blanco, P., Le Seyec, J., Ducret, T., Counillon, L.*, et al.* (2011). The naturally processed CD95L elicits a c-yes/calcium/PI3K-driven cell migration pathway. PLoS Biol *9*, e1001090.

Thomas, S.M., and Brugge, J.S. (1997). Cellular functions regulated by Src family kinases. Annu Rev Cell Dev Biol *13*, 513-609.

Touil, Y., Igoudjil, W., Corvaisier, M., Dessein, A.F., Vandomme, J., Monte, D., Stechly, L., Skrypek, N., Langlois, C., Grard, G.*, et al.* (2014). Colon cancer cells escape 5FU chemotherapy-induced cell death by entering stemness and quiescence associated with the c-Yes/YAP axis. Clin Cancer Res 20, 837-846.

Vaira, V., Faversani, A., Dohi, T., Maggioni, M., Nosotti, M., Tosi, D., Altieri, D.C., and Bosari, S. (2011). Aberrant overexpression of the cell polarity module scribble in human cancer. Am J Pathol 178, 2478-2483.

von Nandelstadh, P., Ismail, M., Gardin, C., Suila, H., Zara, I., Belgrano, A., Valle, G., Carpen, O., and Faulkner, G. (2009). A class III PDZ binding motif in the myotilin and FATZ families binds enigma family proteins: a common link for Z-disc myopathies. Mol Cell Biol 29, 822-834.
Wan, X., Yeung, C., Heske, C., Mendoza, A., and Helman, L.J. (2015). IGF-1R Inhibition Activates a YES/SFK Bypass Resistance Pathway: Rational Basis for Co-Targeting IGF-1R and Yes/SFK Kinase in Rhabdomyosarcoma. Neoplasia 17, 358-366.

Williams, J.C., Weijland, A., Gonfloni, S., Thompson, A., Courtneidge, S.A., Superti-Furga, G., and Wierenga, R.K. (1997). The 2.35 A crystal structure of the inactivated form of chicken Src: a dynamic molecule with multiple regulatory interactions. J Mol Biol 274, 757-775.

Won, S.J., and Martin, B.R. (2018). Temporal Profiling Establishes a Dynamic S-Palmitoylation Cycle. ACS Chem Biol 13, 1560-1568.

Wu, M., Pastor-Pareja, J.C., and Xu, T. (2010). Interaction between Ras(V12) and scribbled clones induces tumour growth and invasion. Nature 463, 545-548.

Xi, L., Schmidt, J.C., Zaug, A.J., Ascarrunz, D.R., and Cech, T.R. (2015). A novel two-step genome editing strategy with CRISPR-Cas9 provides new insights into telomerase action and TERT gene expression. Genome Biol 16, 231.

Xu, D., Lv, J., He, L., Fu, L., Hu, R., Cao, Y., and Mei, C. (2018). Scribble influences cyst formation in autosomal-dominant polycystic kidney disease by regulating Hippo signaling pathway. FASEB J 32, 4394-4407.

Xu, W., Harrison, S.C., and Eck, M.J. (1997). Three-dimensional structure of the tyrosine kinase c-Src. Nature 385, 595-602.

Yeung, C.L., Ngo, V.N., Grohar, P.J., Arnaldez, F.I., Asante, A., Wan, X., Khan, J., Hewitt, S.M., Khanna, C., Staudt, L.M., et al. (2013). Loss-of-function screen in rhabdomyosarcoma identifies CRKL-YES as a critical signal for tumor growth. Oncogene 32, 5429-5438.

Young, L.C., Hartig, N., Munoz-Alegre, M., Oses-Prieto, J.A., Durdu, S., Bender, S., Vijayakumar, V., Vietri Rudan, M., Gewinner, C., Henderson, S., et al. (2013). An MRAS, SHOC2, and SCRIB complex coordinates ERK pathway activation with polarity and tumorigenic growth. Mol Cell 52, 679-692.

Zaal, E.A., and Berkers, C.R. (2018). The Influence of Metabolism on Drug Response in Cancer. Front Oncol 8, 500.

Zahreddine, H., and Borden, K.L. (2013). Mechanisms and insights into drug resistance in cancer. Front Pharmacol 4, 28.

Zeller, C., and Brown, R. (2010). Therapeutic modulation of epigenetic drivers of drug resistance in ovarian cancer. Ther Adv Med Oncol 2, 319-329.

Zhan, L., Rosenberg, A., Bergami, K.C., Yu, M., Xuan, Z., Jaffe, A.B., Allred, C., and Muthuswamy, S.K. (2008). Deregulation of scribble promotes mammary tumorigenesis and reveals a role for cell polarity in carcinoma. Cell 135, 865-878.